

Transport in Relaxation Semiconductors

W. van Roosbroeck and H. C. Casey, Jr.

Bell Telephone Laboratories, Murray Hill, New Jersey 07974

(Received 13 May 1970; revised manuscript received 24 September 1971)

Dielectric relaxation time greater than diffusion-length lifetime τ_0 defines the relaxation semiconductor, typical examples of which include high-resistivity wide-energy-gap crystals as well as amorphous materials. Exploratory analysis which extends earlier linear theory is given for carrier transport in the nonlinear large-signal case. A principal result is "recombinative space-charge injection": A stable space-charge region of majority-carrier depletion with zero net local recombination can be realized through injection of minority carriers. The analysis and independent considerations show that trapping and recombination are enhanced, centers being unscreened and Coulomb-attractive ones having extremely large "space-filling" cross sections. Measurements made for crucial check of the theory with crystals of high-resistivity n -type GaAs confirm a predicted range of sublinear forward current. With fitting of data, τ_0 is found to be subnanosecond and determined by recombination in very deep acceptor centers. Many amorphous semiconductors may be expected to have a Fermi level pinned at the position for minimum (p -type) conductivity simply through the recombination statistics, and so have a negative Hall coefficient. The electronic switching and charge storage in certain heterojunctions and the threshold switching in amorphous materials are considered from the viewpoint of the relaxation case, a unifying principle.

I. INTRODUCTION AND DISCUSSION

In analysis of carrier transport in semiconductors, the assumption of local space-charge neutrality often provides theoretical results consistent with experiment, and many widely used expressions implicitly invoke this assumption. In an analysis of transport with space charge,¹ solutions of the differential equations were shown to be of two principal and fundamentally different types largely according to whether dielectric relaxation time τ_d is smaller than *diffusion-length lifetime*²⁻⁴ τ_0 or exceeds it.⁵ The familiar type is that for $\tau_0 \gg \tau_d$; local space-charge neutrality can then be a good approximation. For $\tau_d \gg \tau_0$, the solutions are drastically different and not in accord with the usual qualitative concepts. Regions of near-zero net local recombination may occur instead, with enhanced space charge whose decay depends on dielectric relaxation. A new regime of semiconductor behavior may be ascribed to $\tau_d \gg \tau_0$. This case may be called that of the *relaxation semiconductor*, or the *relaxation case*, and the familiar one, the *lifetime case*.⁴ Typical examples of a relaxation semiconductor are high-resistivity wide-energy-gap crystalline materials and the amorphous alloys. This paper gives some results of a theoretical investigation of the nonlinear large-signal relaxation case.⁶ It also describes measurements, on minority-carrier injection in crystals of high-resistivity GaAs, that were made for a crucial check of the theory and which confirmed predicted behavior.⁶ Recent further study of the p - n junction characteristics has verified theory in detail.⁷

Small-signal relaxation-case solutions¹ were

derived for the one-dimensional drift without trapping from a pulse of electron-hole pairs injected within an infinite semiconductor.⁸ These show that distributions result which together exhibit *reverse drift*, or drift in the majority-carrier direction. The distributions for electrons and for holes ultimately take the form of continuous doublet distributions of carrier excess and carrier depletion that correspond to a Gaussian distribution of locally reduced field. The doublet separation is equal to the distance electrons and holes drift apart in lifetime τ_0 . The distributions are such that there is excess of one carrier where there is depletion of the other.⁹ The majority-carrier excess and depletion are the greater, and at each point there is a near-zero net recombination or generation, rather than near-zero space charge. The distributions spread through diffusion and through a field-induced pseudodiffusion and decay not with a time constant equal to the lifetime τ_0 , but with the larger time constant τ_d . Since zero net local recombination implies excess electron and hole concentrations of opposite sign, there is *charge separation*, and space charge is enhanced rather than neutralized.

Theory for the large-signal relaxation case is given in Sec. II. Zero net local recombination rate \mathcal{R} is established as the characteristic approximation for $\tau_d \gg \tau_0$ from the fundamental equations. Then, particular heuristic techniques are used to obtain approximate steady-state solutions and gain understanding of essential aspects of the nonlinear transport. Solutions for equal mobilities and no trapping provide correct qualitative conclusions. Their derivation is such that extension to the more general case, which entails significant modifica-

tions, is then readily accomplished.

A principal result in this large-signal theory is *recombinative space-charge injection*: Through carrier injection, the characteristic approximation of zero \mathcal{R} can actually be realized in a stable steady-state space-charge region. Minority-carrier injection can accordingly give substantial depletion of majority carriers. The space charge may be largely that of fixed charges: ionized donors or acceptors that have become uncompensated and any traps that have become occupied. This depletion effect is directly connected with $\mathcal{R}=0$. With Boltzmann statistics, the product np of the electron and hole concentrations then equals its thermal-equilibrium value, the square of the intrinsic concentration, $n_0 p_0 = n_i^2$. In terms of excess concentrations Δn and Δp , it follows that $n_0 \Delta p + p_0 \Delta n + \Delta n \Delta p$ is zero. Then, an injected steady-state electron concentration Δn gives $\Delta p = -p_0 \Delta n / (n_0 + \Delta n)$. In a p -type semiconductor with $p_0 \gg n_0$, for example, $\Delta p \approx -p_0$, or substantially complete depletion of majority carriers, thus results for Δn after recombination that need merely be large compared with the equilibrium concentration n_0 . This major effect, essentially nonlinear and large signal,¹⁰ can occur whether or not there is trapping; but $\Delta n \gg n_0$ may require an initial injected electron concentration not just larger than p_0 , but larger than p_0 plus an appreciable concentration of traps that become occupied. Note also that even large-signal Δp after recombination can give only comparatively small reduction in n , whose initial value is $n_0 \ll p_0$. Thus, for the time-dependent case of the injected neutral pulse, these considerations confirm that reverse drift¹ is also a general property of relaxation semiconductors that applies with trapping as well: The pulse that drifts in the majority-carrier direction is much the less attenuated and provides a direct indication of conductivity type.

With $\tau_d \gg \tau_0$, minority carriers injected from a forward-biased junction or *injector* recombine beyond the low-conductivity region of the junction before their charge can be neutralized through dielectric relaxation. They extend this region, rather than produce the electron-hole excess¹¹ of the lifetime case. Suddenly applied and sufficiently large forward bias may be expected to give current that decreases from its initial value and asymptotically approaches a smaller steady-state current. This decrease is the opposite of what takes place in the lifetime case. An anomalous dependence of differential capacitance on bias may also be expected. The steady current is usually limited largely by space charge of fixed charges and its dependence on bias is then sublinear.

The depletion occurs as a bulk effect in homogeneous semiconductors.¹² Its space charge includes a contribution from the injected minority carriers

which may be minor. This space charge is to be distinguished from that established through reverse bias of a rectifying contact, minority-carrier injection in the presence of which has been investigated.^{13,14} It differs of course from mobile-carrier space charge. With this the current is superlinear, as it is in many different cases of injection which have been analyzed in detail.¹⁵⁻²³ The present theory is a two-carrier theory with a characteristic space charge: Nonequilibrium concentrations generally almost nowhere in the volume give electrical neutrality. Except in the case of ideally uniform optical generation, this is the behavior with transport after transit time (or elapsed time for a transient) of the order of lifetime.

The theory shows that under sufficient forward bias a *depletion drift region* occurs in which diffusion is negligible and depletion is pronounced, with carrier concentrations of the order of the intrinsic concentration. In a sufficiently long diode, the depletion drift region ends in a *recombination front*, in which conductivity about equals that of the (p -type) semiconductor of minimum equilibrium conductivity, and electrons and holes recombine with drift currents about equal. This front separates the depletion region from a region of compensating majority-carrier space charge that reduces the field to its unmodulated value. The length of the region is then proportional to current, and the potential drop, to the square of this length or of the current, and hence there is a range of forward current proportional to about the square root of voltage and independent of diode length. This sublinear dependence is characteristic of the relaxation case. In contrast, in the lifetime case there may be exponential increase of current with forward bias of a junction,¹¹ or voltage-squared dependences from space charge of mobile carriers or from trapping.¹⁵⁻²³ The sublinear range beyond an initial Ohmic range was observed, as described in Sec. III, with n -type crystals of relaxation-case GaAs.

If there is no trapping, the length x_m of the depletion drift region is essentially the distance majority carriers drift in time τ_d under a field equal to the maximum local field that corresponds to minimum conductivity. As field and current increase, x_m may approach τ_d times a velocity of the order of thermal velocity. This x_m for no trapping can be quite large, being about 300 cm for the τ_d of the GaAs described in Sec. IIIA. With trapping, however, the space charge in the region may be mainly that of traps that become occupied. Drift mobility and x_m are then reduced by a trapping factor N_t about equal to the ratio of the concentration n_t of these traps to the concentration of majority carriers. The value of N_t calculated from the present data is of order 10^5 , and the reasonably short 5×10^{-2} -cm diode of Sec. III suffices

for depletion regions not significantly limited by diode length. Values of N_t larger than 10^5 may often be expected.

The relaxation-case forward characteristic has an extended Ohmic range, a *kink voltage*²⁴ V_k for the sublinear threshold of about 13 V being observed.^{6,7} This value agrees with theoretical estimate in Sec. IIE3 of V_k for a junction with extrinsic material equal to about eight times the band-gap potential. In the Ohmic range, forward current is largely diffusive at the edge of the depletion region in which traps are filled by minority carriers, and this region is essentially the equilibrium region not appreciably extended.

An analysis given shows that the length of the recombination front is about equal to the separation from which electrons and holes will drift together during a lifetime τ_0 . It is a fraction α of x_m of order $N_t\tau_0/\tau_d$, and $\alpha \ll 1$ holds because of $\tau_d \gg \tau_0$ if N_t is not too large. A sublinear range implies small α directly. Usually $N_t \gg 1$ also holds. Then, τ_0 determined by recombination in the traps is found to imply a recombination coefficient for minority carriers large compared with the Langevin expression^{25,26} for diffusion-limited capture by Coulomb-attractive centers. This result applies regardless of whether lifetime is determined primarily by electron capture or by hole capture. In crystalline materials, the extremely large capture cross section whose radius is half the average trap spacing usually satisfies the inequality. The concept thus emerges of a "space-filling" cross section, under the assumption of trap spacing large compared with a mean free path. This cross section may also for other reasons usually be expected to apply at low fields in relaxation semiconductors dominated by traps that outnumber majority carriers. For the GaAs crystals, it is found to be about $0.3 \mu^2$, much larger than the cross sections of a square Ångstrom unit or so typical of traps in the lifetime case. Relaxation-case cross sections for capture of majority carriers by neutral centers that are comparatively very large may usually be expected also. It appears that the relaxation case tends to be in part self-realizing because trapping and recombination are characteristically altered in a way that makes τ_0 quite small. The recombination centers in the GaAs are found to be very deep acceptors, at about the intrinsic energy level or above this level. The intrinsic level gives $\tau_0 \approx 2 \times 10^{-10}$ sec. But any level above the Fermi level gives $\tau_0 \approx 1.2 \times 10^{-11}$ sec, and the centers, whose ionized concentration is about $5 \times 10^{12}/\text{cm}^3$, may then be nearly all neutral.

A double-injection negative resistance was observed^{6,7} beyond the sublinear range. This effect, which characteristically involves increase of life-

times with injection level to values at least comparable with the transit time, has been studied in detail.^{18,20} Approximate local neutrality may then apply, since $\mathcal{R} = 0$ does not. The present theory is primarily for "long" transit times in the relaxation case. Double-injection or short-transit-time oscillation, negative resistance, switching, and related photoconductive effects have been described for diodes of compensated high-resistivity Si, Ge, and GaAs doped with deep-level impurities.^{20,27-30} As transit times were decreased and approached lifetimes, currents proportional to about the cube of voltage were generally observed, beyond which the oscillations took place. The theory for this behavior has been given.³⁰ A sublinear current range preceding oscillations was, however, also observed.³¹

The sublinear range has also been reported for *p*-type crystals of trigonal Se.³² In this work, characteristics of the type observed were also obtained by computer. For the computation, models were selected for cases of high-resistivity impurity-compensated semiconductors, and equality of capture and release rates in acceptor-type centers was in effect assumed separately for electrons and for holes.³³ The models thus imply the relaxation case and apply strictly provided there is no recombination front. The boundary conditions assumed in each case appear consistent with this requirement: Transition to the unmodulated semiconductor was apparently ruled out by the assumed fairly large fixed minority-carrier concentrations at the contacts in conjunction with the specified length. Also, since both In and noninjecting Ni contacts gave about the same Ohmic ranges, the Se may well have been nearly minimum-conductivity material, and the sublinear range a result of trapping of electrons without appreciable depletion of holes.

The relaxation case may be expected whenever a sufficiently short lifetime τ_0 occurs in conjunction with sufficiently high resistivity. Reducing temperature sufficiently will reversibly convert many lifetime-case materials to the relaxation case. For a dielectric constant of 12, the dielectric relaxation time in seconds is about 10^{-12} times the resistivity in Ω cm. Thus, with τ_0 equal to 10^{-8} sec, a resistivity somewhat higher than $10^4 \Omega$ cm would be required. At room temperature, such conditions may be met with Si, and are usually readily met with GaAs, GaP, and other semiconductors whose energy gaps are appreciably wider than about 1 eV. Although difficult to determine with any precision in GaAs and GaP, τ_0 is generally less than 10^{-8} sec in these materials. Since most studies have not utilized GaAs or GaP in the high-resistivity range,³⁴ the lifetime case rather than the relaxation case is the one that has

most usually been observed with crystals of these or any semiconductors. The amorphous materials,³⁵⁻⁴² however, are quite generally relaxation semiconductors; through short-range order, an energy-band model applies, though with certain significant modifications. Typical of many are high, near-intrinsic resistivities that are generally not very impurity sensitive, and very short carrier lifetimes with pronounced trapping that strongly limits drift mobilities. In materials that can also have a crystalline form, resistivities are usually orders of magnitude higher than for the crystals, and conductivity band gaps are wider. Amorphous covalent alloys may, for reasons given in Sec. IIE 3 that emerge from the trapping theory, be expected to be minimum-conductivity or maximum-resistivity (*p*-type) materials for given conductivity band gap, and so have negative Hall coefficients. Disordered semiconductors are qualitatively somewhat similar to the amorphous ones, and means for producing relaxation semiconductors might include subjecting crystals to beams of neutrons, electrons, or other radiation.

Not treated here in detail are the photoeffects, which may be expected to differ in various respects from those of the lifetime case. Uniform photoconductivity in trap-dominated relaxation semiconductors is, until nearly all the charged minority-carrier traps are filled, generally due to majority carriers. If photoexcitation in the relaxation case involves transport with separation of electrons and holes, then a space-charge photovoltage results. With a *p-n* junction, it may be possible to realize the comparatively large open-circuit photovoltage corresponding to a given junction current. Such junction photovoltage would be related to forward current not increasing rapidly with bias and the rather long high-resistance junction region. The widely observed larger-than-band-gap "anomalous" photovoltages between the ends of illuminated, non-uniformly thin, evaporated and generally amorphous semiconductor films⁴³ should certainly be considered in the context of relaxation-case transport: They may well be essentially space-charge photovoltages in the present sense, aside from the experimental and theoretical complexities.

That the definition of the relaxation semiconductor serves as a unifying principle for various switching and charge-storage effects⁴⁴ is another theoretical aspect whose detailed treatment is beyond the present scope. In particular, application of concepts of relaxation-case transport leads to the conclusion that the switching to low resistance at a threshold field in certain amorphous semiconductors is due primarily to recombinative space-charge injection of minority electrons.^{44,45} With an illustrative model that applies to some

covalent alloys, the exponential increase of current with field below the threshold is associated with increase in concentration and effective drift mobility of holes activated into extended states of essentially constant microscopic velocity. During the characteristic delay time at the threshold, largely thermal activation of remaining holes may occur through rise in temperature. After all holes are activated, very rapid switching occurs through the injection of electrons to which velocity saturation also applies, and a recombination front is established at the anode.^{44,45} Relaxation semiconductors lend themselves to electronic storage of a simple and fundamental type: Because of charge separation, carriers of one polarity may readily be injected while the compensating charge is switched to an insulated electrode on the surface. The injected carriers can then form a *charge junction*: They can remain for a long time near the electrode in a distribution which is essentially the same as that in an abrupt *p-n* junction at equilibrium.^{44,45} A related case is the following: Certain heterojunctions under sufficient reverse bias exhibit an electronic and reversible switching to a low-resistance state that persists under no bias for weeks, while sufficient forward bias can restore the initial high resistance.^{46,47} This reverse-bias switching is attributed to recombinative space-charge injection of holes, with the low-resistance memory a charge-junction storage effect: The discontinuity initially in the valence-band edge at the interface is shifted by the injected space charge to the conduction-band edge and holds compensating charge of electrons. The conduction is then entirely by holes, in the thin epitaxial *n*-type layer as well as in the *p*-type substrate.^{44,45}

The recombinative space-charge injection considered common to the switching in the amorphous as well as heterojunction cases is a typical relaxation-case transport behavior that can occur under a wide variety of conditions. With sufficient bias, this injection tends to take place so that ultimately a region dominated by minority carriers largely or wholly occupies the injected semiconductor: With increasing current during the transient, the minority-carrier region exhibits growth which is in a sense self-enhanced by the near-minimum conductivity which obtains, even with very-large-signal injection, at the leading edge, where most of the recombination takes place.

II. THEORY

A. Preliminary Formulation for Constant Mobilities

If total current density is known, the transport without trapping involves three dependent variables, which may be two concentration variables and the field \vec{E} . In this case, three differential equations are to be satisfied.⁴⁸

Poisson's equation in its general form includes changes $\Delta\hat{p}$ and $\Delta\hat{n}$ in concentrations of fixed charges:

$$\text{div}\vec{E} = \frac{4\pi e}{\epsilon}(p + \hat{p} - n - \hat{n}) = \frac{4\pi e}{\epsilon}(\Delta p + \Delta\hat{p} - \Delta n - \Delta\hat{n}). \quad (1)$$

Here \hat{p} and \hat{n} are concentrations of fixed positive and negative charges, such as ionized donors and acceptors. Note that the net fixed-charge concentration ($\hat{p} - \hat{n}$) is zero only for the intrinsic semiconductor,⁴⁹ while trapping is present if \hat{p} or \hat{n} is not constant and departs from its thermal-equilibrium value.

Continuity equations are

$$\begin{aligned} \frac{\partial p}{\partial t} &= -e^{-1} \text{div}\vec{I}_p - \mathcal{R} + \Delta g, \\ \frac{\partial n}{\partial t} &= e^{-1} \text{div}\vec{I}_n - \mathcal{R} + \Delta g, \end{aligned} \quad (2)$$

in which \mathcal{R} and Δg are net nonequilibrium inter-band recombination and volume generation rates, and \vec{I}_p and \vec{I}_n are the hole and electron current densities

$$\begin{aligned} \vec{I}_p &= e\mu_p p \vec{E} - eD_p \text{grad}p, \\ \vec{I}_n &= e\mu_n n \vec{E} + eD_n \text{grad}n. \end{aligned} \quad (3)$$

The total current density \vec{I} is the sum of \vec{I}_p , \vec{I}_n , and the displacement current density, and is also given by the curl of the magnetic field:

$$\vec{I} = \vec{I}_p + \vec{I}_n + \frac{\epsilon}{4\pi} \frac{\partial \vec{E}}{\partial t} = \frac{c}{4\pi} \text{curl}\vec{H}. \quad (4)$$

Now, $\text{div}\vec{H}$ is zero and $\text{curl}\vec{H}$ without applied magnetic field must be small, since, with cgs units, c in Eq. (4) is the speed of light. Negligible magnetic field is thus generally associated with the transport itself. It follows that the field \vec{E} generally has substantially zero curl; it always has zero curl in the steady state. It is, therefore, the negative gradient of a potential V and represents a single dependent variable. Also, it follows with Eqs. (1) and (2) from Eq. (4) that $\text{div}\vec{I}$ is zero.

For transport in one Cartesian dimension then, \vec{I} can depend only on time. In general, with \vec{I} known, the expression for it serves one differential equation. Poisson's equation is another. An independent third equation that takes recombination into account results if the continuity equations are added. These equations clearly suffice if there is no trapping; then $\Delta\hat{p}$ and $\Delta\hat{n}$ are zero.

For trapping, it will suffice to consider in detail the formulation for acceptor-type traps in which recombination occurs at a single energy level. With Boltzmann statistics, trapped electron concentration \hat{n} satisfies

$$\frac{\partial \hat{n}}{\partial t} = C_n [n(\mathcal{X} - \hat{n}) - n_1 \hat{n}] - C_p [p\hat{n} - p_1(\mathcal{X} - \hat{n})], \quad (5)$$

in which \mathcal{X} is concentration of the traps, n_1 and p_1 the electron and hole concentrations if the Fermi level were at the energy level of the traps, and C_n and C_p the recombination coefficients for electrons and for holes. In the steady state, the recombination rate is

$$\begin{aligned} \mathcal{R} &= C_i (np - n_i^2) + C_n [n(\mathcal{X} - \hat{n}) - n_1 \hat{n}] \\ &= C_i (np - n_i^2) + C_p [p\hat{n} - p_1(\mathcal{X} - \hat{n})]. \end{aligned} \quad (6)$$

Here, C_i applies to direct electron-hole recombination, and the two forms for \mathcal{R} indicate that the steady-state excess of electron capture rate over emission rate equals the same quantity for holes, in accord with Eq. (5). If various kinds of traps are present, this equality will hold for each kind. Eliminating the trapped electron concentration from Eqs. (6) gives

$$\mathcal{R} = \{C_i + [\tau_{p0}(n + n_1) + \tau_{n0}(p + p_1)]^{-1}\} (np - n_i^2), \quad (7)$$

with $\tau_{p0} \equiv (C_p \mathcal{X})^{-1}$ and $\tau_{n0} \equiv (C_n \mathcal{X})^{-1}$. For traps of more than one kind, \mathcal{R} still has $(np - n_i^2)$ as factor; it is easily seen that the coefficient of this factor then includes a sum of similar terms for each kind.

The relaxation-case approximation for zero Δg of $\mathcal{R} = 0$ therefore implies

$$np = n_i^2 \quad (8)$$

for nondegenerate semiconductors, regardless of whether or not or to what extent there is trapping. Where this approximation holds, the differential equation involving \mathcal{R} may be replaced by Eq. (8). The current densities may be written in terms of the electrochemical potentials,

$$\varphi_p \equiv V + (kT/e) \ln(p/n_i), \quad \varphi_n \equiv V - (kT/e) \ln(n/n_i), \quad (9)$$

as

$$I_p = -e\mu_p p \text{grad}\varphi_p, \quad I_n = -e\mu_n n \text{grad}\varphi_n. \quad (10)$$

Equation (8) is equivalent to φ_p and φ_n having a common value, here called the *relaxation potential* φ_R ,

$$\varphi_R = \varphi_p = \varphi_n. \quad (11)$$

The single potential φ_R determines concentrations of mobile as well as trapped carriers just as the Fermi potential does at equilibrium, and with its gradient, current density as well. Where φ_R applies, it is often useful for qualitative considerations or as a descriptive adjunct to the analysis.

Further formulation will use the recombination rate

$$\begin{aligned} \mathcal{R} &= (np - n_i^2)/(n_0 + p_0) \tau_0 \\ &= (n_0 \Delta p + p_0 \Delta n + \Delta n \Delta p)/(n_0 + p_0) \tau_0, \end{aligned} \quad (12)$$

in which τ_0 is the diffusion-length lifetime.³ This form for \mathcal{R} neglects the concentration dependence of the denominator associated with recombination through centers at specified energy levels, the exact factor multiplying $(np - n_i^2)$ being replaced by its equilibrium value.³ This approximation is here a suitable one: The neglected change in carrier lifetime with injection may, when significant, be taken into account separately. The lifetime τ_0 is defined by

$$\begin{aligned} \tau_0 &= \frac{\tau_{p0}(n_0 + n_1) + \tau_{n0}(p_0 + p_1)}{(n_0 + p_0)} \\ &= \frac{\tau_{tn} \tau_{tp}(n_0/\tau_{tn} + p_0/\tau_{tp})}{(n_0 + p_0)}, \end{aligned} \quad (13)$$

where τ_{tn} and τ_{tp} are the electron and hole capture times. This lifetime may, in principle, be realized as the decay time constant for mobile carriers following a pulse of uniform small-signal⁵⁰ optical generation.⁵¹ For \mathcal{R} small, τ_0 may, in general, be realized in this way with a short pulse.³ Indeed, as the first of Eqs. (13) shows, τ_0 is formally the same as the common lifetime for electrons and holes in the limit of small \mathcal{R} . The definition of τ_0 by Eqs. (13) for arbitrary \mathcal{R} , for which lifetimes are generally quite different, embodies broader physical significance. Consider, for example, deep traps in the *minority-carrier trapping range*.³ This range is defined by a capture rate n_0/τ_{tn} or p_0/τ_{tp} for majority carriers that is the smaller.⁵² If nearly all of the injected minority electrons are quickly trapped and the pulse duration is long compared with this transient, then the subsequent decay is limited by the equilibrium capture rate p_0/τ_{tp} of holes. This rate must be in balance with an equilibrium recombination rate of electrons. For this example, the second of Eqs. (13) gives $p_0/\tau_{tp} = n_0/\tau_0$. Similarly, τ_0 is simply τ_{tn} if holes are quickly trapped. Thus, τ_0 is essentially the equilibrium minority-carrier lifetime that corresponds to the rate that limits or controls recombination.

B. Formulation for Equal Mobilities and No Trapping

It is convenient to employ the concentration variables m and q or Δm and Δq defined by

$$m \equiv \frac{1}{2}(p + n), \quad \Delta m \equiv m - m_0 = \frac{1}{2}(\Delta p + \Delta n), \quad (14)$$

$$q \equiv \frac{1}{2}(p - n), \quad \Delta q \equiv q - q_0 = \frac{1}{2}(\Delta p - \Delta n),$$

in which subscript zero denotes the equilibrium value. For no trapping, Poisson's equation is

$$\Delta q = (\epsilon/8\pi e) \operatorname{div} \vec{E}, \quad (15)$$

and Eqs. (2)–(4) give, for equal mobilities,

$$\vec{I} = 2e\mu \left(m \vec{E} - \frac{kT}{e} \operatorname{grad} q \right) + \frac{\epsilon}{4\pi} \frac{\partial \vec{E}}{\partial t} \quad (16)$$

and

$$\frac{\partial m}{\partial t} = -\mu \operatorname{div} \left(q \vec{E} - \frac{kT}{e} \operatorname{grad} m \right) - \mathcal{R} + \Delta g, \quad (17)$$

in which μ is the common mobility and the diffusivities have been replaced by $kT\mu/e$. The recombination rate of Eqs. (12) in the variables of Eqs. (14) is

$$\begin{aligned} \mathcal{R} &= (m^2 - q^2 - n_i^2)/2m_0 \tau_0 \\ &= [(m_0 + \frac{1}{2} \Delta m) \Delta m - (q_0 + \frac{1}{2} \Delta q) \Delta q] / m_0 \tau_0. \end{aligned} \quad (18)$$

Equations (16) and (17) show that for equal mobilities, \vec{I} includes the currents of oppositely moving carriers, namely, the conductivity drift current and the space-charge-inbalance diffusion current, while the net recombination in the steady state is given by the divergence of a current consisting, so to speak, of carriers that move together.

To facilitate quantitative conclusions, the three differential equations will be written in dimensionless form. The Debye length

$$L_D \equiv (kT\epsilon/8\pi e^2 m_0)^{1/2} \quad (19)$$

will be used as the length unit for dimensionless distance, with respect to which GRAD and DIV will be used to denote the gradient and divergence operators. The concentration unit m_0 will be used, and dimensionless field

$$\vec{F} \equiv e \vec{E} L_D / kT. \quad (20)$$

Then, with $\Delta Q \equiv \Delta q / m_0$, Poisson's equation, Eq. (15), assumes the simple form

$$\Delta Q = \operatorname{DIV} \vec{F}. \quad (21)$$

With $U \equiv t/\tau_d$ time in units of the dielectric relaxation time,

$$\tau_d \equiv \epsilon/8\pi e\mu m_0 = \epsilon/4\pi\sigma_0, \quad (22)$$

where σ_0 is the equilibrium conductivity, Eq. (16) becomes

$$\vec{F}_a \equiv \vec{F} M - \operatorname{GRAD} \Delta Q + \frac{\partial \vec{F}}{\partial U}. \quad (23)$$

Here M is m/m_0 and

$$\vec{F}_a \equiv e \vec{I} L_D / kT \sigma_0 \quad (24)$$

is the dimensionless total current density, equal to the dimensionless asymptotic field for total current density \vec{I} in the unmodulated semiconductor with equilibrium conductivity σ_0 . With \mathcal{R} given by Eq. (18), Eq. (17) becomes

$$\frac{\partial \Delta M}{\partial U} = -\text{DIV}(Q\vec{F} - \text{GRAD}\Delta M) - \frac{\tau_d}{\tau_0} [\frac{1}{2}(M^2 - Q^2 - N_i^2) - \Delta G], \quad (25)$$

in which ΔM is $\Delta m/m_0$, Q is q/m_0 , N_i is n_i/m_0 , and ΔG is given by

$$\Delta G \equiv \Delta g \tau_0 / m_0. \quad (26)$$

Note that Eqs. (14) and the definitions of M and Q give

$$P \equiv p/m_0 = M + Q, \quad N \equiv n/m_0 = M - Q, \quad (27)$$

and $(M^2 - Q^2)$ is equal to NP .

C. Relaxation Hyperbola

The choice made of L_D and τ_d as length and time units is the natural one when these units exceed the diffusion length and lifetime.⁵³ It results in the factor τ_d/τ_0 on the right-hand side of Eq. (25). The expression in brackets this factor multiplies is the dimensionless excess of recombination rate over generation rate. For $\tau_d \gg \tau_0$, the approximation of setting this expression equal to zero, which is not to be taken to imply that the entire term in Eq. (25) is zero or necessarily small, gives

$$\begin{aligned} \frac{1}{2}(NP - N_i^2) &= \frac{1}{2}(M^2 - Q^2 - N_i^2) \\ &= (1 + \frac{1}{2}\Delta M)\Delta M - (Q_0 + \frac{1}{2}\Delta Q)\Delta Q \\ &= \Delta G, \end{aligned} \quad (28)$$

in which

$$Q_0 \equiv (p_0 - n_0)/(p_0 + n_0) = \pm(1 - N_i^2)^{1/2} \quad (29)$$

is the equilibrium value of Q , the upper and lower signs on the right-hand side applying for p and n type, respectively. The relationship of Eq. (28) defines the *relaxation hyperbola*, the locus of $\mathcal{R} = \Delta g$ in the concentration plane. For $\Delta g = 0$, this hyperbola implies the relaxation potential φ_R and conversely. Each point on it then corresponds to a value of φ_R as well as to a certain thermal-equilibrium conductivity of the semiconductor of given n_i .

The factor τ_d/τ_0 may be accounted for by considering the simple case of suddenly applied uniform interband generation or constant ΔG and no transport. Then Eq. (25) shows that τ_d/τ_0 in effect changes the dimensionless time variable from U to τ/τ_0 , or time in units of lifetime. That is, positive ΔM appears so that the expression in brackets goes to zero with time constant about τ_0 , as expected. No space charge appears in this case; ΔQ stays equal to zero.

Figure 1 shows a relaxation hyperbola plotted in the ΔM - ΔQ plane. This is one for p -type material that is not very strongly extrinsic, and for $\Delta G = 0$, or no volume generation. The N and P axes are asymptotes of the hyperbola. At the vertex, here

called the *conversion point*, electron and hole concentrations are equal. For zero ΔG , the conversion-point concentration equals the intrinsic concentration n_i , and the hyperbola passes through the ΔM - ΔQ origin, which corresponds to thermal equilibrium. The conversion point separates the hyperbola into two branches: On *branch I*, minority carriers predominate, and on *branch II*, which includes the origin, majority carriers predominate. A solution in one dimension for the relaxation case usually amounts to a mapping against distance or time of a segment of the relaxation hyperbola, and in the nonequilibrium steady state, this segment is, as will be seen, largely confined to one of the branches. A solution may also involve points off the hyperbola, as when a recombination front is present.

Where the hyperbola applies, it is a locus of stability: Any departure from it disappears through rapid recombination or generation. The horizontal arrow in Fig. 1 represents a transition to a point of majority-carrier depletion on the hyperbola through recombination without trapping of injected minority carriers. Sudden unipolar injection of electrons in specified initial concentration over a specified volume in the p -type semiconductor is assumed. Initially, the injected electrons give (negative) space charge and enhanced conductivity corresponding to some point on the line $\Delta Q = -\Delta M$. With $\tau_d \gg \tau_0$, conductivity given by ΔM will de-

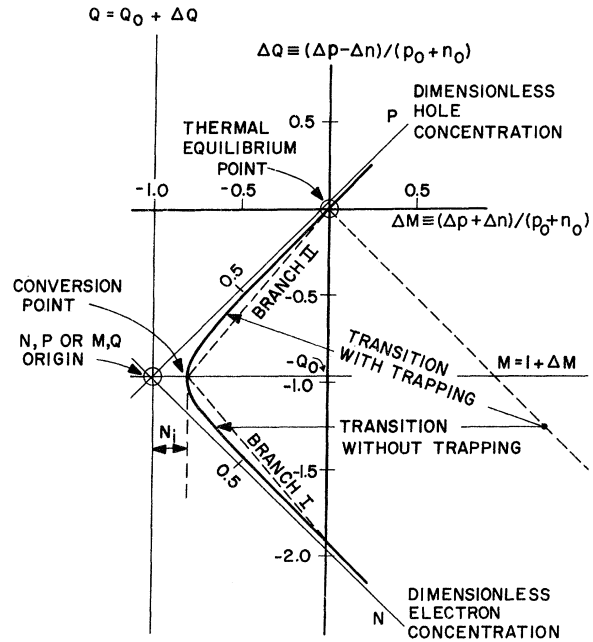


FIG. 1. Relaxation hyperbola. Recombinative transitions of injected minority carriers and the line approximation employed are shown. A p -type semiconductor with hole-electron concentration ratio p_0/n_0 of 100 is assumed.

crease rapidly through recombination while mobile-carrier space charge given by ΔQ remains virtually unchanged. If the injected electron concentration is larger than the equilibrium hole concentration, then the transition occurs to a point on branch I; otherwise there is transition to a point on branch II. If initial electron concentration exceeds $2Q_0$ times m_0 , or about twice the equilibrium hole concentration, then there is transition to a point on branch I corresponding to enhanced conductivity, or $\Delta M > 0$; otherwise there is conductivity depletion. The arrow directed upward in the figure shows schematically the effect of minority-carrier trapping on the transition. As shown in Sec. II E 1 and Appendix B, there is a decrease in this case in the magnitude of ΔQ , since the trapping causes a smaller final contribution to space charge from mobile minority carriers. An injected initial concentration that may be considerably larger is then required for transition to branch I. With trapping, the actual path for the transient generally departs markedly from the straight arrow. If electrons are rapidly trapped, the path is along the dashed line to near the origin and then curves downward, becoming nearly parallel to the P axis as holes ultimately recombine.

Large-signal conductivity depletion proceeds with increasing time constant and generally takes much longer than τ_0 . From Eq. (7), the final time constant τ'_0 may be estimated as the decay time for equal virtual small-signal⁵⁰ concentration increments δn and δp above the final concentration n'_0 and p'_0 . This is the diffusion-length lifetime for the semiconductor with equilibrium concentrations changed to n'_0 and p'_0 . Under the approximation of Eq. (18), τ'_0 is $\tau_0 / [(p'_0 + n'_0) / (p_0 + n_0)] = \tau_0 / M'_0 \gg \tau_0$, the inequality applying for $M'_0 \ll 1$, or pronounced depletion. But local dielectric relaxation time τ'_d is also increased, and in exactly the same ratio for equal mobilities. For $M'_0 > 1$, τ'_0 and τ'_d are similarly decreased.⁵⁴ The equilibrium ratio τ_d / τ_0 thus holds approximately over the significant portion⁵⁴ of the hyperbola, the effect of unequal mobilities being minor.⁵⁵ That the hyperbola actually applies is due to this circumstance, and its stability is implicit through $\mathcal{R} - \Delta g = 0$, which at the same time is the condition that defines it. Recombinative space-charge injection is accordingly a stable effect, the possibility of whose occurrence depends simply on equilibrium properties.

A semiconductor in the lifetime case at low field will, in fact, not go into the relaxation case at a higher field through increase in τ_d from saturation of carrier velocity. It has been shown¹ in context with derivation of continuity equations that τ_d is the reciprocal of the sum of electron and hole dielectric relaxation frequencies; if there is intervalley scattering, frequencies for each valley are added.

Each frequency, as may be expected, is proportional to the change of velocity with field, or differential mobility. Hence velocity saturation may cause a large increase in τ_d . But theory not included here shows that the significant ratio is actually L_D^2 over the product of diffusivity and τ_0 , which reduces to τ_d / τ_0 for constant mobilities.⁵³

Transient decay after recombinative injection generally takes place ultimately through a recombination front and at a rate controlled by dielectric relaxation. Initial injection over an appreciable volume small compared with the entire volume is assumed. After transition to the hyperbola, each point on it corresponding to a point in the injected volume will eventually move to the ΔM - ΔQ origin or thermal-equilibrium point. For small-signal injection, the time required is of order τ_d . With large-signal depletion, a longer time is required. Dielectric relaxation is then slow within the volume. At the boundary of the volume, there is a recombination front, and the recombination causes the spread and approach to equilibrium of an adjoining region of small-signal depletion in the volume.

The lifetime of carriers of given sign injected into a depletion region is often larger than τ_0 . Under the approximation of Eq. (18), the small-signal hole lifetime is readily found to be $\tau_0 / (n / 2m_0) = \tau_0 / \frac{1}{2}N$, where n is the local electron concentration on the hyperbola. Similarly, the electron lifetime is $\tau_0 / (p / 2m_0) = \tau_0 / \frac{1}{2}P$.

Solving for ΔQ from Eq. (28) gives

$$\Delta Q = -Q_0 \pm [Q_0^2 + (2 + \Delta M)\Delta M - 2\Delta G]^{1/2}. \quad (30)$$

The two branches of the hyperbola join for the radicand in Eq. (30) equal to zero, so that the conversion point is given by

$$M = 1 + \Delta M = (1 - Q_0^2 + 2\Delta G)^{1/2} = (N_1^2 + 2\Delta G)^{1/2} \quad (31)$$

and

$$Q = Q_0 + \Delta Q = 0. \quad (32)$$

Equation (32) implies $n = p$. For $\Delta G = 0$, Eq. (31) gives $M = N_1$, and, with Eqs. (27), it is verified that electron and hole concentrations equal n_1 . With $\Delta G > 0$, the concentrations exceed n_1 at the conversion point, which is then at a larger value of M . The hyperbola then no longer passes through the point of thermal equilibrium. It is further evident from Eq. (31) that if ΔG exceeds $\frac{1}{2}Q_0^2$ at any point, then negative ΔM or depletion of conductivity cannot occur at that point.

Note that Q_0 defined by Eq. (29) is negative for n type. The choice of p type for Fig. 1 and as may be convenient in the analysis implies no substantive restriction. Where a result depends explicitly on the sign of Q_0 , it may readily be modified for n type.

D. Solutions for Equal Mobilities and No Trapping

1. Formulation using Line Approximation

It is suitable to approximate the two branches of the relaxation hyperbola by two straight lines as shown in Fig. 1. These are the lines from the conversion point to the two intercepts on the ΔQ axis of which one is the ΔM - ΔQ origin. These lines for the respective branches are

$$\begin{aligned} \text{I: } \Delta M &= -\lambda_0 - \lambda_1 \Delta Q, & \Delta Q &\leq -Q_0, \\ \text{II: } \Delta M &= \lambda_1 \Delta Q, & \Delta Q &\geq -Q_0, \end{aligned} \quad (33)$$

where λ_0 and λ_1 are defined by

$$\lambda_0 \equiv 2(1 - N_i), \quad \lambda_1 \equiv (1 - N_i)/Q_0. \quad (34)$$

For steady-state transport in the x coordinate direction, it is of advantage to use the field,

$$F = -\frac{dW}{dX}, \quad X \equiv \frac{x}{L_D}, \quad (35)$$

as dependent variable, where

$$W \equiv eV/kT \quad (36)$$

is dimensionless electrostatic potential. Then Eq. (23) becomes

$$\frac{d^2 F}{dX^2} - FM = -F_a. \quad (37)$$

The derivative, the magnitude $\text{GRAD}(\text{DIV } \vec{F})$, enters when ΔQ is eliminated by use of Poisson's equation, Eq. (21). Substituting for $M = 1 + \Delta M$ from Eqs. (33) in Eq. (37) and further eliminating ΔQ gives the differential equations for the two branches,

$$\begin{aligned} \text{I: } \frac{d^2 F}{dX^2} + \lambda_1 F \frac{dF}{dX} + (\lambda_0 - 1)F &= -F_a, \\ \text{II: } \frac{d^2 F}{dX^2} - \lambda_1 F \frac{dF}{dX} - F &= -F_a. \end{aligned} \quad (38)$$

2. p - n Junction at Equilibrium

For zero current, W introduced as an independent variable in Eqs. (38) by use of $dX = -dW/F$ gives equations linear in F^2 , which is then readily found analytically in terms of W . A further quadrature, easily performed numerically, using

$$X = -\int_0^W \frac{dW}{F} \quad (39)$$

gives the dependence of W on X . This dependence so obtained, as well as those of F and M , are shown in Fig. 2 for $p_0 = 100n_0$, which is the rather weakly extrinsic case of Fig. 1. The X and W origins are taken at the conversion point. Solutions for the two branches join there. Figure 2 shows an extended region of appreciable majority-carrier depletion, where the curve for M lies below the

dashed line at ordinate unity. The analysis, an illustrative exercise in the use of the line approximation, is here omitted; a similar exact analysis using the Boltzmann expressions,

$$P = N_i e^{-W}, \quad N = N_i e^W, \quad (40)$$

is as easy. Space-charge concentration in traps may be written as function of W , and its contribution to F^2 also obtained in simple closed form. The details are beyond the present scope.

For a more strongly extrinsic semiconductor, with N_i very small, there is sharper variation of M with distance. About the conversion point or X origin there is a region in X of very small, intrinsic conductivity. A parabolic dependence of W on X is then readily found to obtain in this region, which has nearly uniform space charge. A largely similar result holds if trapping is appreciable, though it is found that concentrations with deep traps may vary comparatively slowly with distance.

If the junction region and semiconductor are illuminated so that ΔG is uniform in the volume, then the solution is the same as that for a semiconductor of increased N_i at equilibrium. It suffices to replace N_i by $(N_i^2 + 2\Delta G)^{1/2}$, which is M at the conversion point. If this M is sufficiently small so that the line approximation may be used, then N_i may be so replaced in the definitions of λ_0 and λ_1 of Eqs. (34). As has been indicated, this M exceeds unity for $\Delta G > \frac{1}{2}Q_0^2$, which is $\Delta g\tau_0 > \frac{1}{4}(p_0 - n_0)^2/(p_0 + n_0)$, and there is then local reduction of total carrier concentration in the junction region without depletion below the equilibrium value. Largely this same result holds even if lifetime depends on Δg through

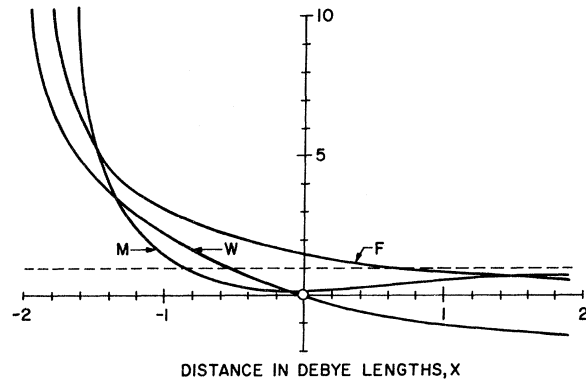


FIG. 2. Relaxation-case semiconductor in equilibrium with a minority-carrier injector; the dependence on distance of dimensionless potential W , field F , and total carrier concentration M . This semiconductor is the p -type one of Fig. 1 for the case of no trapping. Mobilities are assumed equal, so that M represents conductivity. Note the region of conductivity depletion where $M < 1$ holds. The curves apply also for the lifetime case, for which $np = n_i^2$ holds at equilibrium.

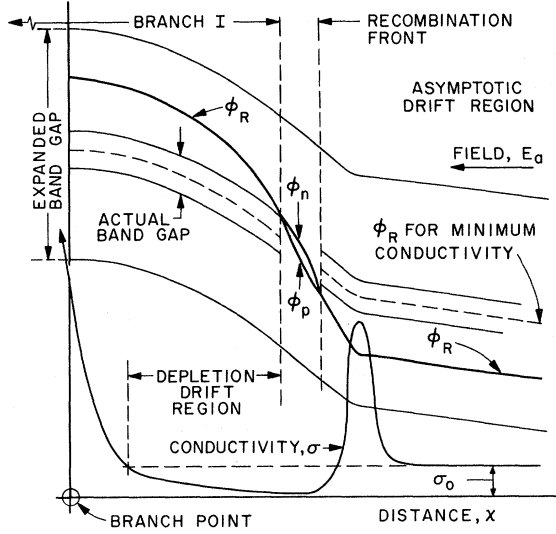


FIG. 3. Long relaxation-case p -type semiconductor with a forward-biased injector contact; the energy-band diagram and conductivity σ . The distance origin has been taken at the branch point; the electron injector is to the left. This case is one with conductivity depletion, and the potential variation is comparatively pronounced in relation to the indicated actual band gap, which has been expanded to show ϕ_R and the recombination front.

minority-carrier trapping that gives extrinsic photoconductivity, as may be seen by use of Eq. (7) for \mathcal{R} .

3. Forward-Biased Junction

The energy-band diagram and dependence of conductivity on distance are shown qualitatively in Fig. 3 for a long p -type semiconductor with the injector contact at the left. The forward bias results in a zero-field point, here also called the *branch point*. This is a singular point of the differential equation, Eq. (37) or its generalization, written with W as independent variable and F^2 as dependent variable; F is taken as the positive root of F^2 to the left of the branch point and as the negative root to the right. At the branch point, there is only diffusion and no contribution of drift to current. If ΔQ_b and W_b are the values of ΔQ and W there, the approximations

$$\begin{aligned}\Delta Q &= \Delta Q_b - F_a X, \\ F &= \Delta Q_b X - \frac{1}{2} F_a X^2, \\ W &= W_b - \frac{1}{2} \Delta Q_b X^2 + \frac{1}{6} F_a X^3\end{aligned}\quad (41)$$

hold in its neighborhood, as is easily found by neglecting the drift term⁵⁷ in Eq. (37).

Under sufficient forward bias, drift rather than diffusion will predominate to the right of some point to the right of the branch point, and particularly

in the region of conductivity depletion, as indicated in Fig. 3. A *depletion drift region* will be established. Solutions for the approximation of drift only are readily obtained. Consider branch I of the hyperbola. From Eq. (37) the approximate differential equation in F is given by

$$FM = F_a \quad (42)$$

with M given for branch I by

$$M = 1 - \lambda_0 - \lambda_1 \frac{dF}{dX}, \quad (43)$$

from Eqs. (21) and (33). The solution in terms of M is, for forward bias or $F_a < 0$,

$$\lambda_0(Z-1) - \ln Z = \frac{(\lambda_0-1)^2}{\lambda_1} \frac{(X-X_1)}{|F_a|}, \quad (44)$$

where Z is defined by

$$Z = \lambda_0^{-1} + (1 - \lambda_0^{-1})M^{-1}. \quad (45)$$

Here X_1 is the X at which $M=1$ holds, or the total concentration, largely of minority electrons on branch I, equals the total equilibrium concentration. The plane of the injector is quite near X_1 and choice of X_1 as distance origin gives simple results.⁵⁸

The distance of the conversion point from the origin is, as will be shown, the approximate length of the depletion drift region. This distance X_c in Debye lengths may be found by setting M equal to N_i in Eq. (45). The result from Eq. (44) is then

$$\frac{(\lambda_0-1)^2}{\lambda_1} \frac{X_c}{|F_a|} = \frac{(1-N_i)(1-2N_i)}{N_i} - \ln \frac{1}{2N_i}. \quad (46)$$

It is easily seen from Eqs. (19) and (20) that $X_c/|F_a|$ equals $x_c/\mu|E_a|\tau_d$, or the actual distance x_c measured in units of the *relaxation drift length* $\mu|E_a|\tau_d$, which is the distance a carrier drifts under field E_a in the dielectric relaxation time. If $N_i \ll 1$ holds, then Eq. (46) is approximately

$$x_c/\mu|E_a|\tau_d = 1/N_i \gg 1. \quad (47)$$

This result shows that if forward bias is sufficient for a majority-carrier depletion region in which drift predominates, then this region extends over a number of relaxation drift lengths.

For $N_i = 0.01$, the M and F/F_a calculated from Eqs. (42), (44), and (45) are shown in Fig. 4. For this case, x_c equals 96 relaxation drift lengths, and there is substantial majority-carrier depletion over most of this distance. For $N_i = 0.2$, the more weakly extrinsic case of Fig. 1, x_c equals about 3.4 relaxation drift lengths, with $M \approx N_i$ over a distance of order one length. The relaxation drift length is, however, proportional to τ_d , and τ_d equals $(\sigma_m/\sigma_0)\tau_m$, with τ_m the dielectric relaxation

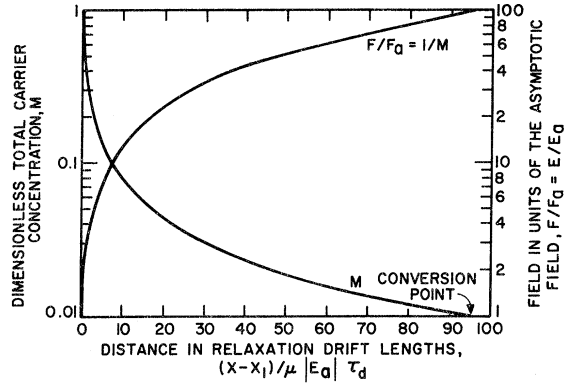


FIG. 4. Depletion drift region; dependence on distance of dimensionless total carrier concentration M and field in units of asymptotic field. Equal mobilities and a p -type semiconductor with $N_i = 0.01$ and thus $p_0/n_0 = 4 \times 10^4$ are assumed.

time for minimum conductivity σ_m , which is here intrinsic, so that σ_m/σ_0 is N_i . Indeed, considering E_a fixed and semiconductors that differ only in conductivity, x_c is only some 40% larger for $N_i = 0.01$ than for $N_i = 0.2$. To the approximation of Eq. (47), x_c is independent of N_i or conductivity, being given by

$$x_c = \mu |E_a| \tau_m = \mu |E_m| \tau_d. \quad (48)$$

Here $E_m \equiv I/\sigma_m$ is the field attained at the end of the depletion region. This largest field is $\tau_m/\tau_d \equiv \sigma_0/\sigma_m$ times E_a . For no trapping, the length of the depletion region is thus the distance carriers drift in time τ_d under the field E_m . It is proportional to the maximum (here intrinsic) resistivity times the asymptotic field.

Self-consistency of this analysis will now be demonstrated by deriving a condition that is met when a depletion drift region occurs. It will be shown later in this section that for this case of equal mobilities the region is confined to branch I of the relaxation hyperbola; its approximate boundary is the minimum-conductivity point, which for equal mobilities is the conversion point.

The magnitude of $\Delta Q < 0$ decreases as branch I is traversed towards the conversion point with increasing X . From Eq. (23) or Eq. (37), the diffusion term $d\Delta Q/dX$ positive implies $|F_a| > |F|M$. The drift approximation requires that ΔQ change sufficiently slowly with X so that $|F|M$ may be set equal to $|F_a|$. The average $\langle d\Delta Q/dX \rangle$ of the diffusion term over the range of the drift solution is easily calculated, and this must be small compared with $|F_a|$. From Eq. (47), the dimensionless distance X_c for $N_i \ll 1$ is $\mu |E_a| \tau_m/L_D$, and in X_c , the change in ΔQ is from $-2Q_0$ to $-Q_0$ or equal to $Q_0 \approx 1$. Hence when the drift solution applies the inequality in

$$\left\langle \frac{d\Delta Q}{dX} \right\rangle = \frac{1}{X_c} = \frac{L_D}{\mu |E_a| \tau_m} \ll |F_a| = \frac{e |E_a| L_D}{kT} \quad (49)$$

holds, which gives the condition

$$V_a \equiv \mu E_a^2 \tau_m \gg kT/e. \quad (50)$$

The defined potential V_a , here called the *injection potential*, equals $|E_a| x_c$ and is large compared with the Boltzmann potential. A qualitative physical interpretation is that V_a , an effective potential based simply on $|E_a|$, is smaller than the actual potential, and so takes account of field being smaller than $|E_a|$ in part of the region towards the injector where conductivity (due to injected minority carriers) is of order σ_0 and larger. Very moderate asymptotic fields suffice, for this case of no trapping, if maximum resistivity and hence τ_m are not too small: For example, with $\mu = 10^3$ cm²/V sec as an order-of-magnitude value for (electron or hole) mobility, the condition is readily met in GaAs or in Si by $|E_a|$ respectively of the order of 1 V/cm or about 30 times larger than this.

Over a large part of the depletion drift region for equal mobilities, the field exceeds the asymptotic field by a factor not much less than N_i^{-1} , the factor that applies at the conversion point. Voltage rise to this point (from the point at which $M = 1$ holds) should therefore be nearly V_a/N_i . An analytic solution shows that this value is too large by just a factor of 2.

This solution for electrostatic potential in the depletion drift region follows from

$$W = - \int F dX, \quad dX = -\lambda_1 dF / (M + \lambda_0 - 1). \quad (51)$$

The second equation is tantamount to Eq. (43) and holds for branch I. With Eq. (42), Eqs. (51) give

$$W = \lambda_1 \int \frac{F^2 dF}{F_a + (\lambda_0 - 1)F}, \quad (52)$$

and if W equals zero for $M = 1$, the integral is

$$W = [\lambda_1 F_a^2 / (\lambda_0 - 1)^3] \left[\frac{1}{2} \lambda_0^2 (Z^2 - 1) - 2\lambda_0 (Z - 1) + \ln Z \right] \quad (53)$$

in terms of M , with Z so given by Eq. (45). This result shows that voltage is proportional to the square of the current provided the entire depletion drift region is contained within the length of the semiconductor. By multiplying both sides of Eq. (53) by N_i/F_a^2 , the voltage is expressed in units of V_a , because $W/F_a^2 = V/\mu E_a^2 \tau_d$ and $\tau_d = N_i \tau_m$. For $N_i \ll 1$, for which $\lambda_0 \approx 2$ and $\lambda_1 \approx Q_0 \approx 1$ hold, the voltage so expressed is

$$V/V_a = N_i [2(Z - 1)^2 + \ln Z], \quad (54)$$

with Z given by

$$Z = \frac{1}{2}(M^{-1} + 1) \quad (55)$$

from Eq. (45). The expression on the right-hand side of Eq. (54) simplifies to $(2N_i)^{-1}$ for $M=N_i$, and this gives the potential drop V_c from the conversion point in units of V_a .

The condition, Eq. (50), that is met when there is a depletion drift region specifies sufficiently large E_a or current density. The equivalent condition in terms of actual potential drop is thus

$$V_c = V_a/2N_i \gg (2N_i)^{-1}kT/e. \quad (56)$$

Application of this equation requires, in principle, that voltage across the region be known or estimated.

How the depletion drift region ends depends on what boundary conditions are specified. It should first be noted that for equal mobilities the region does not extend beyond the conversion point. Beyond the conversion or minimum-conductivity point on branch II, M or conductivity increases, and Eq. (42) then requires that $|F|$ decreases. But since ΔQ is negative, $|F|$ must increase according to Poisson's equation, Eq. (21). This contradiction shows that, with steady forward current, branch II beyond the minimum-conductivity point is inaccessible from branch I. The depletion drift region is, in principle, realizable up to this point, since it may be terminated at the corresponding location by a "matching" electrode, one that does not perturb the space charge.⁵⁹ The region may also be thought of as being joined at that location to a length of intrinsic or minimum-conductivity material terminated by an Ohmic contact. This boundary condition is consistent with the drift approximation in that the field at the junction is continuous there. The discontinuity in space charge under the approximation would be removed by diffusion, since (with equal mobilities) ΔQ occurs only in the diffusion term of the current equation. Space charge would thereby be perturbed over a small distance of the order of only one diffusion length.⁶⁰ In the case of the long or unterminated semiconductor under forward bias, Poisson's equation requires a region of positive space charge between the depletion drift region and the asymptotic drift region, as is shown in Fig. 3. This space charge is due to mobile holes, and reduces field to its asymptotic value E_a . It must, therefore, in total amount equal the total negative space charge in the entire depletion drift region from the point in that region at which conductivity and local field are equal to their asymptotic values. Over-all neutrality applies, and it is in part as if the mobile holes were simply displaced away from the injector contact. Both field and concentration gradient contribute to a steady flow of holes back towards the depletion drift region.

According to familiar lifetime-case concepts, such adjoining steady regions of opposite space charge would of course not occur. Their occurrence in the

relaxation case is connected with the *recombination front* between them. In Appendix A, the approximate consistency of $\mathfrak{R}=0$ with the recombination equation is shown to fail short of the minimum-conductivity point. The location x_R at which the recombination front starts is found to be given by

$$x_c - x_R \approx \mu |E_a| \tau_0 / 2N_i = \frac{1}{2} \mu |E_m| \tau_0 \quad (57)$$

for $N_i \ll 1$, no trapping, and equal mobilities. This result gives the approximate length of the recombination front, and comparison with Eq. (47) shows that it occupies in this case a fraction about $\tau_0/2\tau_d \ll 1$ of the depletion drift region. This region should, therefore, be realizable in the long semiconductor as well, terminating there in a relatively narrow front in which electron and hole currents are approximately equal to the equal minimum-conductivity drift currents. In the front, diffusion may actually predominate since ΔQ changes rapidly with distance and the term $d\Delta Q/dX$ may be large. But drift predominates if current density is sufficiently large so that $\mu E_a^2 \tau_0 \gg 2N_i kT/e$ holds. This condition resembles that of Eq. (50) for the depletion drift region, but calls for a current larger by the factor $(2\tau_d/\tau_0)^{1/2}$. It is based on $|F_a|$ large compared with $d\Delta Q/dX$ approximated as L_D divided by the length of the front, over which the change in ΔQ is of order unity.

E. Extension for Trapping and Unequal Mobilities

1. Trapping and Recombinative Transition

The pronounced steady depletion of majority carriers through recombination will occur when concentration of mobile injected minority carriers appreciably exceeds the equilibrium value. An analysis given in Appendix B shows that trap filling to a concentration in excess of the *capture concentration*³

$$\mathfrak{N}^* \equiv \mathfrak{N} (\hat{n}_0/\mathfrak{N})(1 - \hat{n}_0/\mathfrak{N}) \quad (58)$$

is required. Now, \mathfrak{N}^* is small if the traps are nearly all empty or nearly all filled at equilibrium, and has a largest value $\frac{1}{4}\mathfrak{N}$ for traps half-filled. It follows that if the traps are normally either mostly filled or mostly empty, then the depletion can be realized without much effect on trap occupation. Some effects of trapping on transition to the hyperbola are also analyzed in Appendix B. It is shown that a transition to branch II like the one of Fig. 1 entails a reduction in the magnitude of ΔQ approximately by the trapping factor

$$N_i^* \equiv 1 + \mathfrak{N}^* / (p_0 + n_0). \quad (59)$$

Also, for transition to branch I, the initial electron concentration must meet the approximate condition,

$$\Delta n_1 > (p_0 - n_0) N_i^*, \quad (60)$$

which is essentially that Δn_1 must exceed $p_0 + \mathfrak{K}^*$.

2. Extension for Depletion Drift Region

With the technique of the line approximation, solutions of Sec. IID 3 are readily extended. Equations (33) and (34) for the lines still hold as written in terms of ΔQ , but the more general Poisson's equation,

$$\Delta Q = \frac{1}{2} \Delta \hat{N} + \frac{dF}{dX}, \quad \Delta \hat{N} \equiv \Delta \hat{n} / \frac{1}{2} (p_0 + n_0) \quad (61)$$

must be used. On branch I, completely filled traps or $\Delta \hat{n} \approx (\mathfrak{K} - \hat{n}_0)$ may be assumed, since $n > n_i \gg n_0$ holds there for extrinsic p -type material.⁶¹ This assumption holds also past the conversion point along part of branch II, further along which $\Delta \hat{n}$ approaches zero. Then Eq. (61) results in simple modification of Eqs. (33) and (34): For branch I, λ_0 is replaced by the expression of Eq. (34) plus $\frac{1}{2} \lambda_1 \Delta \hat{N}$. With unequal mobilities also taken into account, the expressions for both λ_0 and λ_1 are easily modified for each of the branches, and immediate generalization follows in this way of the entire formalism of Sec. IID 3 for the simple case.

For unequal mobilities, the dimensionless current equation, Eq. (23), is replaced by

$$\bar{F}_a \Sigma_0 = \bar{F} \Sigma + \lambda_b \text{GRAD} \Delta M - \text{GRAD} \Delta Q + \frac{\partial \bar{F}}{\partial U}, \quad (62)$$

in which

$$\Sigma \equiv M - \lambda_b Q \quad (63)$$

is the dimensionless conductivity and $\Sigma_0 = 1 - \lambda_b Q_0$ its equilibrium value, with

$$\lambda_b \equiv (\mu_n - \mu_p) / (\mu_n + \mu_p), \quad (64)$$

where μ_n and μ_p are the mobilities. Note that λ_b does not exceed unity. For steady drift only in the x direction, Eq. (62) reduces to

$$F \Sigma = F_a \Sigma_0, \quad (65)$$

and, with Eq. (61), Σ for branch I is given by

$$\Sigma = 1 - \lambda_0 - \lambda_b Q_0 - \frac{1}{2} (\lambda_1 + \lambda_b) \Delta \hat{N} - (\lambda_1 + \lambda_b) \frac{dF}{dX}. \quad (66)$$

Comparison of Eqs. (42) and (43) with Eqs. (65) and (66) shows that results of Sec. IID 3 pertaining to the depletion drift region may be extended simply by replacing λ_0 by $\lambda_0 + \lambda_b Q_0 + \frac{1}{2} (\lambda_1 + \lambda_b) \Delta \hat{N}$, λ_1 by $\lambda_1 + \lambda_b$, F_a by $F_a \Sigma_0$, and M by Σ , and similarly for branch II, if part of this branch is also involved.

Some principal results so extended will be given for the extrinsic approximation $N_i \ll 1$. Distance, in a depletion drift region from x_1 near the injector at the left where Σ equals Σ_0 to a point where $\Sigma \ll 1$ holds, is given by

$$x - x_1 = \mp (1 \pm \frac{1}{2} \Delta \hat{N})^{-1} (1 \mp \lambda_b) \bar{\mu} E_a \tau_d / \Sigma, \quad (67)$$

with the upper and lower signs applying for p and n type, respectively, and

$$\bar{\mu} \equiv (\mu_p p_0 + \mu_n n_0) / (p_0 + n_0) = \sigma_0 / 2e m_0. \quad (68)$$

As will be shown, the recombination front is at the location of the minimum-conductivity point, defined by $\mu_p p = \mu_n n$ on the hole branch of the hyperbola. Equation (67) applies up to the front; for n type, minimum conductivity occurs on branch I, while for p type, solutions for the two branches that are entirely similar under the extrinsic approximation join at the conversion point. The distance x_m to the front, or length of the depletion drift region, is therefore $x - x_1$ from Eq. (67) when Σ is given its minimum-conductivity value,

$$\Sigma_m = (1 - \lambda_b^2)^{1/2} N_i = 4(\mu_n \mu_p)^{1/2} n_i / (\mu_n + \mu_p) (p_0 + n_0). \quad (69)$$

However, Σ_m may be eliminated by use of $\tau_d / \Sigma_m = \tau_m / \Sigma_0$, where τ_m is the corresponding dielectric relaxation time; note that $1 \mp \lambda_b$ in Eq. (67) is the approximate value of Σ_0 . The trapping factor is

$$N_t \equiv 1 \pm \frac{1}{2} \Delta \hat{N} = \begin{cases} 1 + (\mathfrak{K} - \hat{n}_0) / (p_0 + n_0), & p \text{ type} \\ 1 + \hat{n}_0 / (n_0 + p_0), & n \text{ type} \end{cases} \quad (70)$$

since $\mathfrak{K} - \hat{n}_0$ or \hat{n}_0 is the concentration n_t of traps that become filled by minority carriers. Equation (67) is thus found to give, for either conductivity type,

$$x_m = \bar{\mu} |E_a| \tau_m / N_t = \bar{\mu} |E_m| \tau_d / N_t, \quad (71)$$

where E_m is the field at the minimum-conductivity point. Note the reduction of x_m by the trapping factor, that $\bar{\mu}$ about equals the (microscopic) majority-carrier mobility, and that $\bar{\mu} / N_t$ is the effective drift mobility.

The potential difference across x_m is found to be given by

$$|V_m| = \frac{1}{2} |E_m| x_m = \frac{1}{2} \bar{\mu} E_m^2 \tau_d / N_t = \frac{1}{2} (\sigma_0 / \sigma_m) V_a, \quad (72)$$

where

$$V_a \equiv \bar{\mu} E_a^2 \tau_m / N_t = |E_a| x_m \quad (73)$$

is the injection potential of Eq. (50) redefined more generally with $\bar{\mu} / N_t$. The condition that is met when the depletion drift region occurs is, as before, V_a large compared with the Boltzmann potential. This is derived by specifying relatively small average $\langle d(\lambda_b M - Q) / dX \rangle$ of the diffusion term from the point $\Sigma = \Sigma_0$ on branch I to the minimum conductivity point. With Eq. (72), the condition may be written in terms of the actual potential as

$$|V_m| \gg \frac{1}{2} (\sigma_0 / \sigma_m) kT / e, \quad (74)$$

and holds in this form independently of trapping. Thus, with trapping, essentially the same potential drop is realized over a distance shorter by the factor N_t and with current that is increased by the square root of N_t .

Extended theory for the recombination front is given in Appendix A2. It is shown that the front has fractional length α given by

$$\alpha = \frac{1}{2} [(\mu_n + \mu_p) / \bar{\mu}] N_t' \tau_0 / \tau_d, \quad (75)$$

where

$$N_t' \equiv 1 - \frac{1}{2} \frac{\Delta \hat{N}}{\Delta Q_m} = \begin{cases} 1 + \frac{(\mathfrak{N} - \hat{n}_0)}{p_0 - n_0 - (\mu_n - \mu_p) n_i / (\mu_n \mu_p)^{1/2}}, & p \text{ type} \\ 1 + \frac{\hat{n}_0}{n_0 - p_0 + (\mu_n - \mu_p) n_i / (\mu_n \mu_p)^{1/2}}, & n \text{ type} \end{cases} \quad (76)$$

is a trapping factor. Here $\Delta Q_m \equiv Q_m - Q_0$ is the ΔQ at the minimum-conductivity point. If the material is not too near-intrinsic and the mobility ratio not unusually large,

$$\alpha \approx \frac{1}{4} (1 + \mu_{\min} / \mu_{\text{maj}}) N_t \tau_0 / \tau_d \quad (77)$$

may be a good approximation, where μ_{\min} and μ_{maj} are the minority- and majority-carrier mobilities, since $|\Delta Q_m| \approx 1$ and $N_t' \approx N_t$ then hold and $\bar{\mu}$ is very nearly μ_{maj} . Equation (75) of course gives $\tau_0 / 2\tau_d$ for the case of equal mobilities and no trapping of Sec. IID3. With Eq. (71), the actual length of the front is

$$\alpha x_m = \frac{1}{4} (\mu_n + \mu_p) (N_t' / N_t) |E_m| \tau_0 \approx \frac{1}{4} (\mu_n + \mu_p) |E_m| \tau_0. \quad (78)$$

This is essentially the distance of separation from which electrons and holes will drift together in time τ_0 under the largest local field E_m and does not depend explicitly on trap concentration.

3. Some Consequences of Extended Theory

This section deals mainly with the unusually large trapping cross sections in relaxation semiconductors, with amorphous semiconductors having minimum conductivity, with how the trapping factor and hence concentration of traps that become filled may be determined from the current at the sublinear threshold, and with an estimate of the kink voltage V_k .

The theory of the recombination front leads to the large cross sections. The condition $\alpha \ll 1$ is implied directly by a sublinear range. Then, from Eq. (77), essentially $N_t \tau_0 / \tau_d \ll 1$ must hold, and since $N_t \gg 1$ usually does also, τ_0 / τ_d must be correspondingly quite small. Then, for the case of τ_0 determined by recombination in the traps, a lower limit for the cross section for capture of minority carriers is determined. Assume an n -type semi-

conductor, and consider first equilibrium hole capture rate the larger, which is equivalent to the equality level being between the Fermi level and the conduction band or

$$n^* \equiv C_p p_1 / C_n \gg n_0. \quad (79)$$

From Eq. (13) for τ_0 and Eqs. (70) and (77), $\alpha \ll 1$ is then found to give

$$C_n n_1 \gg \pi e (\mu_n + \mu_p) p_0 / \epsilon, \quad (80)$$

or a lower limit for the electron release frequency, and also

$$C_p \gg C_L \equiv \pi e (\mu_n + \mu_p) / \epsilon, \quad (81)$$

or a lower limit for the recombination coefficient for holes which is C_L , here called the *Langevin recombination coefficient*. With $n_0/p_1 = n_1/p_0$, Eq. (81) follows as a strong condition from Eqs. (79) and (80) together. For the case of equilibrium electron capture rate being larger, $\alpha \ll 1$ simply gives Eq. (81) directly, and not Eq. (80). It is easy to verify that the same results hold in a formal sense for traps of the donor type. But for the GaAs semiconductor described in Sec. IIIA, Eq. (81) gives $C_p \gg C_L = 1.7 \times 10^{-4}$ cm³/sec, or a cross section for hole capture (obtained by dividing by thermal velocity) of order 10^{-10} cm² or larger. Centers with so large a cross section may well be assumed Coulomb attractive and therefore of the acceptor type in an n -type semiconductor.

Equation (81) specifies a minority-carrier recombination coefficient large compared with that for diffusion-limited capture: The familiar Langevin coefficient^{25,26} for such capture is $4\pi e \mu_{\min} / \epsilon$, and C_L is this multiplied by the factor $\frac{1}{4}(1 + \mu_{\text{maj}} / \mu_{\min})$. The physical significance of this factor will be made evident; it is usually of order unity. The cross section $\pi(\frac{1}{2}n_i^{-1/3})^2$ whose radius is half the average spacing between the centers is about the largest possible. For the particular GaAs it is about 3×10^{-9} cm² and meets the condition $\alpha \ll 1$ by more than two orders of magnitude. Independent reasons will be given why such a "space-filling" cross section for minority-carrier capture should obtain quite generally in the trap-dominated relaxation case. For some of these reasons, a very large cross section for majority-carrier capture by neutral centers should also obtain. A C_n that is only about three orders of magnitude smaller than C_p is, indeed, indicated by analysis of data in Sec. III C based on Eq. (80) and approximate equality of (increased) hole lifetime and transit time at the end of the sublinear range.

The Langevin cross section is itself orders of magnitude larger than the cross sections ordinarily encountered in the lifetime case. In a simple derivation²⁶ of the familiar expression for this cross section, the rate at which volume per carrier is

swept out under the central Coulomb field is independent of radial distance r . Spherical symmetry is assumed, so that the recombination coefficient is the area $4\pi r^2$ times the velocity $\mu e/\epsilon r^2$, or $4\pi e\mu/\epsilon$. This independence of r might seem to suggest that no larger recombination coefficient can occur. The formalism does not really imply this, as will now be shown. A property of the Langevin cross section should first be noted. If the radius r is chosen so that the velocity $e\mu/\epsilon r^2$ for this radius equals the thermal velocity v_θ , then the area $4\pi r^2$ is $4\pi e\mu/\epsilon v_\theta$. Since the cross section is the recombination coefficient divided by v_θ , this area is the familiar Langevin cross section. Therefore the microscopic drift velocity extrapolated from constant mobility is v_θ at the *Langevin radius*. At this radius, the central field gives an appreciable contribution to carrier velocity between collisions, or within one mean free path, and a carrier is directed towards the center correspondingly. Such a carrier may be scattered away and another may be drawn towards the center in its stead, and since the capture probability must then be divided between carriers, the formalism with spherical symmetry applies. Hence the Langevin cross section entails not only relatively small mean free path but also the assumption that the center is well surrounded by the carriers it attracts. In contrast, if the concentration of these carriers is of order n_i or less, a condition generally met nearly everywhere (with the trivial exception of a small region adjoining the injector), then the cross section is the space-filling one, being based on the transport of one particular carrier to a center. If a carrier within a free path of the boundary of the volume dominated by a center is scattered out of this volume, it does not in effect escape but enters the volume dominated by a neighboring center, and such scattering occurs with statistical uniformity. Effective escape does occur when the centers are outnumbered by carriers of the same sign, or majority carriers; they are then screened by these carriers and their Coulomb fields are, so to speak, statistically obscured. Cross sections may then be smaller by as much as several orders of magnitude, as in the lifetime case.

The space-filling cross section obtains strictly for zero applied field only. It is otherwise decreased approximately to the cross section determined by the radius at which the central Coulomb field equals the applied field. In a trap-dominated relaxation semiconductor, the *Langevin cross section* C_L/v_θ of the present theory may therefore actually be realized (with a charged center) through saturation of the minority-carrier drift velocity, and at the smallest applied field for this saturation. The factor 4 does not occur in this cross section, π times the square of the Langevin radius for this

case, because spherical symmetry does not apply. Furthermore, the sum of the mobilities in place of minority-carrier mobility reflects in a statistical way drift of an electron and a hole towards each other: As derived, C_L applies to τ_0 , that is, to the entire recombination process. Also, equal and opposite flow densities are actually realized at the recombination front.

When the condition of Eq. (81) is not met there may be an extended recombination front rather than a relatively short one terminating a depletion region with predominant drift. With velocity saturation, the condition may no longer hold. Drift velocity is then constant in magnitude essentially everywhere, and the resultant of the applied and central Coulomb fields establishes its direction at any point. Carriers in this case will mostly drift past centers whose average separation is large compared with two Langevin radii. On the other hand, the condition is not met whenever n_i is sufficiently large so that the space-filling cross section is smaller than the Langevin cross section, as would occur in the particular GaAs for $n_i \approx 10^{16}/\text{cm}^3$. The average radius for v_θ is smaller in this case than the Langevin radius.

Sufficiently large concentrations of recombination centers such that their average separations are less than the mean free paths, as in certain amorphous alloys, may be expected to result in a (*p*-type) semiconductor of minimum conductivity, properly defined by electron and hole flow densities everywhere equal and opposite at low fields. Such a semiconductor is in a sense an extended recombination front in its simplest form. The concentration n_i of ionized minority-carrier traps is compensated by a slightly larger concentration of oppositely ionized majority-carrier traps. Concentrations of these ionized centers of acceptor and donor types may be only small fractions of the respective total concentrations. In any case, there is no screening and carriers are strongly trapped at neutral or ionized centers, with pronounced recombination in and generation from these centers. Carriers emitted and activated into mobile extended states contribute to the equilibrium conductivity. The mean free path is of the order of an electron wavelength or more. An emitted carrier is trapped a free path away, either producing a Coulomb-attractive center of the same polarity or neutralizing one of the opposite polarity, and the probability is not much smaller than unity that it recombines. It remains mobile and unrecombined on the average for only slightly more than a single mean free path. The rates at which electrons and holes are so scattered into a given volume element (physically small but containing many atoms) will be equal because of very short τ_0 and detailed balance. If the difference in effective masses is

neglected, then this equality in rates implies that the total times per unit volume in extended states are also equal, so that holes with the shorter mean free path have proportionately larger concentration. The exact, more purely phenomenological condition is that the concentrations n_0 and p_0 in extended states times the corresponding microscopic diffusivities are equal. With Einstein's relation, this is the equality of the electron and hole conductivities and drift with equal and opposite flow densities at low fields. It is easily seen that the ambipolar Hall coefficient for this p -type case should be negative; it contains the difference $\mu_{pH} - \mu_{nH} < 0$ of the Hall mobilities as factor. This consequence appears to resolve the so-called Hall-effect-Seebeck-effect anomaly for the amorphous materials, with which positive thermoelectric power is observed in conjunction with negative Hall coefficient. The generally rather small magnitude of this coefficient may be largely due to the recombination after single free paths. Note that, as a concept, the detailed-balance pinning of the Fermi level through the recombination provides a new approach. The observed insensitivity of conductivity to addition of impurities is, indeed, one obvious consequence, and very large concentrations of near-midgap centers, for example, need not be invoked. Detailed treatment of this case and consideration of any of the various other cases of large trap concentration in crystalline as well as amorphous materials are beyond the present scope.

The trapping factor N_t and hence the concentration n_t may be determined from the threshold current. Equating the injection potential V_a of Eq. (73) to the Boltzmann potential gives

$$N_t = e \bar{\mu} E_a^2 \tau_m / kT. \quad (82)$$

Here the E_a that should be used is the asymptotic field for a current equal to half the observed threshold current. The reason is as follows: The sublinear dependence of current or E_a on potential given by Eqs. (72) and (73) holds only for values sufficiently above the threshold. A more detailed theory would be required for the sublinear characteristic near the threshold. It is a plausible surmise, supported at least fairly well by data, that the characteristic does not differ much from the law $(I - I_t)/I_t = [(V - V_t)/V_t]^{1/2}$ relating the increments above the threshold, (I_t, V_t) ; it must be between this law and the ratio law, $I/I_t = (V/V_t)^{1/2}$. If the increment law is plotted logarithmically, then it is seen that it gives essentially Ohmic behavior beyond (I_t, V_t) , which is the "actual" or extrapolated threshold defined by the intersection of the Ohmic and limiting half-power ratio-law curves; the apparent threshold or *kink point* (I_k, V_k) is on the Ohmic line extended at $(2I_t, 2V_t)$, or twice the extrapolated threshold. There is a slight super-

linear bump between (I_t, V_t) and (I_k, V_k) , beyond which there is a sublinear dependence of nearly constant but slowly increasing apparent ratio-law exponent whose approximate value over the initial two decades in voltage above threshold is 0.43.

An estimate of the kink voltage V_k follows from approximation of the Ohmic part of the characteristic.⁶² Minimum-conductivity material over the width x_s of a space-charge barrier due to uniform concentration n_t of fixed charges gives

$$|V| = (\sigma_0/\sigma_m) |E_a| x_s, \quad x_s = (\epsilon V_s / 2\pi e n_t)^{1/2}, \quad (83)$$

for the Ohmic line, V_s being the space-charge variation of potential in the barrier; E_a is the current divided by σ_0 and area of cross section. Potential in terms of E_a for the limiting half-power sublinear range is given by Eqs. (72) and (73), and V_k , twice the voltage at the intersection with the line of Eq. (83), is (for $N_t \gg 1$) found to reduce to

$$V_k = 8V_s \approx 8V_b, \quad (84)$$

in which the approximation of V_s by the band-gap potential V_b applies for sufficiently strongly extrinsic material. With intrinsic material, V_k is about $4V_b$. Part of the barrier region near the junction interface has high conductivity, but Eqs. (83) and (84) should be reasonably good approximations, since this part is relatively narrow.

III. EXPERIMENTAL PROCEDURES AND RESULTS

A. Preparation of Diodes

The GaAs samples used in this study were from single-crystal, (100)-oriented wafers obtained from oxygen-doped and compensated crystals grown by the floating-zone technique. Hall and resistivity measurements showed that these wafers are n type with a room-temperature carrier concentration of $3.0 \times 10^{17}/\text{cm}^3$, resistivity of $4.6 \times 10^7 \Omega \text{ cm}$, and mobility of $4.5 \times 10^3 \text{ cm}^2/\text{V sec}$. They were polished with a bromine-methanol etch that provides a damage-free surface.

The p - n junctions were formed at a depth of about 3μ by diffusion of Zn at 650°C for 8 h. Individual wafers, of diameter approximately 0.250 in. and 0.02 in. thick, were sealed in a fused silica ampoule along with a 5, 50, and 45 at. % Ga, As, and Zn diffusion source.⁶³ This diffusion source was used because it reproducibly gives planar junctions and prevents changes in resistivity and carrier concentration that frequently occur during diffusion with other sources and diffusion conditions. The surface concentration with this source is about $1.7 \times 10^{20}/\text{cm}^3$, and the Zn concentration decreases abruptly below concentrations of about $10^{19}/\text{cm}^3$. The diffused layer was removed from one side of each wafer by lapping, and a thin In and Au layer was evaporated on the lapped side to

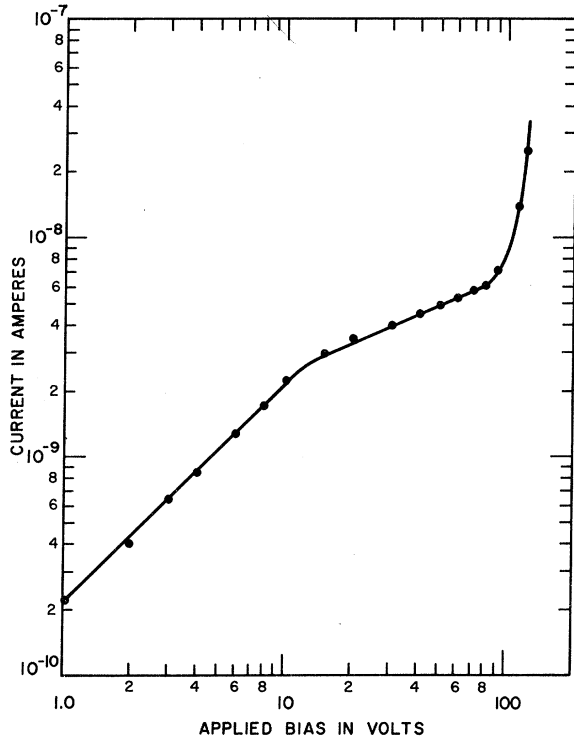


FIG. 5. Forward current-voltage characteristic of a single-crystal n -type GaAs diode. The negative-resistance portion of the characteristic is not shown.

provide an Ohmic contact. The In-Au ratio was about 10:1 by weight, and enough In was used to provide about a 2300-Å layer. The In was evaporated first and then the Au. The layer was then alloyed by heating to 550 °C. Contact to the p -type layer was provided by sputtering 1500 Å of Ti and 3000 Å of Pt. A 0.8–1.0- μ layer of Au was evaporated on the Pt. Each wafer was then cut into approximately 30-mil squares, and lightly etched to remove the saw damage. The squares were bonded to headers with Au-20%-Sn preforms, and Au wires were bonded to the Au layer on the p^+ surface.

B. Electrical Measurements

Current-voltage characteristics were determined with the mounted samples in a light-tight enclosure. The voltage was supplied by either a Hewlett-Packard 611A or Keithley 241 digital voltage supply. The current was measured with a Hewlett-Packard 425A ammeter. A typical room-temperature⁶⁴ characteristic is shown in Fig. 5. As shown in this figure, current varies linearly with voltage from a low value (actually 10^{-11} A at 0.04 V) up to 13 V and then varies sub-linearly with voltage.⁶⁵ The dependence in the sub-linear range is approximately $I = I_t(V/V_t)^{0.44}$, and

at a bias of 80 V the sub-linear range ends. At about 120 V a negative-resistance range (not shown in the figure) was observed to start.

C. Analysis and Discussion

The Ohmic line in Fig. 5 gives a resistance of $4.8 \times 10^9 \Omega$, while the bulk resistivity over the total length of 4.5×10^{-2} cm and for the cross section of 4×10^{-3} cm² gives a calculated resistance of $5.2 \times 10^6 \Omega$, nearly an order of magnitude smaller. Most of the resistance is therefore junction resistance near the injector contact. An intrinsic concentration⁶⁶ n_i of $9 \times 10^5/\text{cm}^3$ at 295 °K and a mobility ratio of 20 give $N_t \approx 2n_i/(n_0 + p_0) = 6 \times 10^{-2}$, $\lambda_b = 0.9$, intrinsic resistivity ρ_1 of $1.5 \times 10^9 \Omega \text{ cm}$, and maximum resistivity $\rho_m = (1 - \lambda_b^2)^{-1/2} \rho_1$ of $3.5 \times 10^9 \Omega \text{ cm}$. Thus the observed junction resistance equals the resistance of minimum-conductivity material at 295 °K over a length $L_D/13.5 = 5.6 \times 10^{-3}$ cm; with $\epsilon = 12.5$ for GaAs, the Debye length L_D from Eq. (19) is 7.6×10^{-2} cm. This fraction of L_D seems reasonable with trapping, and it provides an estimate of the extent of the junction region.

The observed kink voltage V_k of about 13 V is approximately the theoretical estimate $8V_b$ of Eq. (84). The observed exponent of 0.44 for the sub-linear range is in perhaps fortuitously close agreement with the theoretical exponent 0.43 for the increment law given in Sec. II E 3. This agreement supports the estimate of N_t by use of Eq. (82) with E_a the asymptotic field for half the kink current I_k . With $I_k = 2.7 \times 10^{-9}$ A, this E_a is 15.6 V/cm and gives $N_t \approx 1.7 \times 10^5$ and thus $n_t \approx \hat{n}_0 \approx 5.1 \times 10^{12}/\text{cm}^3$ for the concentration of traps that become filled by holes. The space-filling cross section is about 2.7×10^{-9} cm². With the value of N_t , effective drift mobility is about 2.6×10^{-2} cm²/V sec, and the length x_m of the depletion drift region calculated from Eq. (71) increases in proportion to current to 6.9×10^{-3} cm at 80 V. This x_m added to the estimated length of the junction region gives 1.25×10^{-2} cm. The average field at this bias is 1800 V/cm, and the calculated largest field, the product of $E_a = 69$ V/cm and $\sigma_0/\sigma_m = 75$, is nearly 3 times larger. Electron velocity in GaAs saturates, however, with maximum velocity at about 3000 V/cm. Beyond the recombination front, the space charge of electrons is as a result progressively spread out with increasing bias so as to support uniform current, while the field there increases. This field and the recombination-front field both approach the velocity-saturation field as depletion rapidly spreads. At 80 V, depletion with increased hole lifetime extends to the end contact. As indicated also by potential-probe measurements, an associated rapid increase in hole concentration therefore probably causes the initial increase in current above 80 V, and current in this range is

then space-charge limited.⁷ The negative resistance above 120 V is then of the double-injection type.^{7,18,20} Because transit times in this range are not long compared with the lifetimes, this is not specifically a relaxation-case effect. Note that since the average field is 2400 V/cm at 120 V, increased concentration of electrons injected from the end contact, where the field is largest, results in part from velocity saturation.

The cross section for electron capture or the electron emission rate may be estimated by use of the assumption that lifetime and transit time of holes are equal at the end of the sublinear range. Since the traps are filled with holes, lifetime is limited by the rate $C_n n \mathcal{X}$ of electron capture by the (neutral) centers. Towards the end contact, minimum-conductivity electron and hole concentrations n_m and p_m give the recombination rate $C_n n_m \mathcal{X}$ and $\Delta p = p_m - p_0$, and, therefore, the hole lifetime $(p_m - p_0)/C_n n_m \mathcal{X} = [(p_m - p_0)/n_m] \tau_{n0}$. With $\mu_p = 225$ cm²/V sec, the hole transit time at 80 V is about 10^{-7} sec. Equating the two times gives $\tau_{n0} \approx 5.6 \times 10^{-9}$ sec. Then $\tau_{n0}^{-1} = (1 + n_1/n_0) C_n \hat{n}_0$ from the equilibrium statistics relates C_n and n_1 . In particular, if $n_1 \ll n_0$ is assumed, then C_n is 3.5×10^{-5} cm³/sec, while $n_1 \gg n_0$ gives $C_n n_1 = 1.05 \times 10^3$ /sec for the electron emission rate and smaller C_n . The largest possible cross section from C_n for electron capture by a neutral center is therefore some three orders of magnitude smaller than the space-filling cross section for Coulomb-attractive hole capture.

Further conclusions about the recombination model and estimates of τ_0 now follow from $\alpha \ll 1$. This condition and Eqs. (79)-(81) are tantamount to $C_p \gg (1 + n^*/n_0) C_L$, which gives $n^*/n_0 = C_p \rho_0 / C_n n_1 \ll 1.55 \times 10^2$, or $C_n n_1 \gg 4.7$ /sec. Thus, with the C_n for $n_1 \ll n_0$, the condition gives $n_1 \gg 1.3 \times 10^5$ /cm³, or n_1 at least of order $n_i = 9 \times 10^5$ /cm³. That is, the acceptor centers must be very deep ones whose energy level is at the intrinsic level or above this level. Equation (13) for $n_0 \gg p_0$ may be written as $\tau_0 = (C_p \hat{n}_0)^{-1} (1 + n^*/n_0)$, and $\tau_0 \approx 2 \times 10^{-10}$ sec follows if the energy level is assumed to be the intrinsic level. The centers are mostly ionized, with $n_0 = 0.97 \mathcal{X}$, if at this level; and, with $n^*/n_0 = 24$, this τ_0 is determined by capture of majority electrons. However, $n_1 \gg n_0$ or the energy level above the Fermi level gives the fixed electron emission rate and $\tau_0 \approx 1.2 \times 10^{-11}$ sec. Then $n^*/n_0 \approx 0.7 \approx 1$ holds, which implies that the centers are in the *recombination range* but essentially at a boundary of this range that corresponds to the "equality level": The (equal) capture and emission rates for holes very nearly equal these rates for electrons. Since n_1 may exceed n_0 by orders of magnitude in this case, $\mathcal{X} \gg \hat{n}_0 = 5.1 \times 10^{12}$ /cm³ or centers nearly all neutral may obtain. With comparatively many

neutral acceptor centers and with p_0 three orders of magnitude smaller than n_0 , recombination involving the donor centers, which are mostly neutral midgap centers from oxygen, probably does not affect τ_0 appreciably.

ACKNOWLEDGMENTS

We are much indebted to T. M. Buck, who was instrumental in starting the experimental effort and to which he made early contributions, and to H. J. Queisser for his encouraging enthusiasm and significant contributions that started with collaboration during the summer of 1970. Discussions with C. G. B. Garrett led to the extension for trapping, and we are indebted for various helpful comments also to J. A. Burton, A. R. Hutson, M. Lax, and especially G. K. Wertheim, who followed the work with stimulating and continued interest.

APPENDIX A: THEORY FOR RECOMBINATION FRONT

1. No Trapping and Equal Mobilities

Equation (25), the recombination equation, written for steady drift in one dimension and zero ΔG is

$$-\frac{d}{dX}(QF) = \frac{1}{2} \frac{\tau_d}{\tau_0} (M^2 - Q^2 - N_i^2). \quad (85)$$

With no diffusion, M may be expressed in terms of F by use of Eq. (42). If F is introduced in place of X as independent variable⁶⁷ by use of Eq. (21), Poisson's equation, then Eq. (85) becomes

$$-\Delta Q \left(F \frac{dQ}{dF} + Q \right) = \frac{1}{2} \frac{\tau_d}{\tau_0} \left[\left(\frac{F_d}{F} \right)^2 - Q^2 - N_i^2 \right]. \quad (86)$$

In this nonlinear differential equation, it is permissible to linearize the departure in ΔQ from its value $\Delta \bar{Q}$ for $\mathcal{R} = 0$, since slight net recombination or generation will produce comparatively large changes in the divergence of QF . Write for ΔQ ,

$$\Delta Q = \Delta \bar{Q} + (\tau_0/\tau_d) \Delta Q_1, \quad (87)$$

and note that adding Q_0 gives Q . To the first order in $\tau_0/\tau_d \ll 1$, Eq. (86) gives

$$\Delta Q_1 = \Delta \bar{Q} \left(1 + \frac{d \ln \bar{Q}}{d \ln F} \right) = -\frac{\Delta \bar{Q} N_i^2}{Q^2}, \quad (88)$$

or

$$\Delta Q = \Delta \bar{Q} [1 - (\tau_0/\tau_d) N_i^2/\bar{Q}^2]. \quad (89)$$

The second form for ΔQ_1 in Eq. (88) readily follows from the right-hand member of Eq. (86) being zero for $Q = \bar{Q}$, the bar denoting the value for $\mathcal{R} = 0$.

The relaxation hyperbola applies if ΔQ very nearly equals $\Delta \bar{Q}$. From Eq. (89), the condition for

this is

$$\tau_0/\tau_d \ll \bar{Q}^2/N_i^2 = \bar{M}^2/N_i^2 - 1. \quad (90)$$

Since \bar{M} and \bar{Q} are, respectively, N_i and zero at the conversion point, this condition must fail short of this point. Equation (89) shows that, as the conversion point is approached, ΔQ exhibits departure from $\Delta\bar{Q}$ with rapid decrease in magnitude, as is consistent with space charge going to zero. The path in the ΔM - ΔQ plane clearly lies to the right of the relaxation hyperbola, which implies a region of net recombination in which $\Re > 0$ holds. This region is the recombination front.

The fraction of the depletion drift region the front occupies may be estimated by defining its boundary by

$$\bar{M} = (1 + \alpha)N_i, \quad 0 < \alpha \ll 1 \quad (91)$$

with \bar{M} such that

$$\tau_0/\tau_d = \bar{Q}^2/N_i^2 \quad (92)$$

holds, for which ΔQ as given by Eq. (89) is zero. Equations (91) and (92) and the equation (in \bar{M} and \bar{Q}) for the hyperbola give

$$\alpha \approx \tau_0/2\tau_d. \quad (93)$$

The solution of Eqs. (44) and (45) then furnishes the distance between the boundary x_R of the recombination front for which Eqs. (91)–(93) hold and the conversion point. This distance is given by

$$\frac{(\lambda_0 - 1)^2}{\lambda_1} \frac{X_c - X_R}{|F_a|} = \frac{1 - 2N_i}{N_i} \frac{\alpha}{1 + \alpha} - \ln \frac{(1 + \alpha)(1 - N_i)}{1 - N_i + \alpha N_i} \\ \approx \frac{(1 - 2N_i)^2}{1 - N_i} \frac{\alpha}{N_i}, \quad (94)$$

or, for $N_i \ll 1$, by

$$\frac{x_c - x_R}{\mu |E_a| \tau_d} \approx \frac{\alpha}{N_i} \approx \frac{\tau_0}{2N_i \tau_d}. \quad (95)$$

Comparison of this result with Eq. (47) shows that α is the fraction of the depletion drift region the recombination front occupies.

2. Extended Recombination—Front Theory

With trapping, the general Poisson's equation, Eq. (61), must be used, and unequal mobilities require generalization of the recombination equation, Eq. (25). It is easily seen that in this equation $\partial \Delta M / \partial U$ is replaced by $\partial(\Delta M + \lambda_b \Delta Q) / \partial U$, while the divergence term is multiplied by the reciprocal of

$$K \equiv \frac{1}{2} [1 + (\mu_p^2 p_0 + \mu_n^2 n_0) / \mu_n \mu_p (p_0 + n_0)] \\ \approx \frac{1}{2} (1 + \mu_{\max} / \mu_{\min}), \quad (96)$$

in which the approximation applies for suitably ex-

trinsic material. In the steady state, τ_d/τ_0 is in effect multiplied by K . The extended form of Eq. (86) is thus

$$-(\Delta Q - \frac{1}{2} \Delta \hat{N}) \left(F \frac{dQ}{dF} + Q \right) = \frac{1}{2} \frac{K \tau_d}{\tau_0} (M^2 - Q^2 - N_i^2). \quad (97)$$

The linearization

$$\Delta Q = \Delta \bar{Q} + (\tau_0/K\tau_d) \Delta Q_1 \quad (98)$$

is appropriate. Since specifying the value of the independent variable F for given total current density now fixes the value of Σ (rather than M), Eq. (98) implies, from Eqs. (63) and (65), the corresponding linearization

$$M = \bar{M} + (\lambda_b \tau_0/K\tau_d) \Delta Q_1. \quad (99)$$

Equations (97)–(99) give

$$\Delta Q_1 = \Delta \bar{Q} \left(1 - \frac{\Delta \hat{N}}{2\Delta \bar{Q}} \right) \left[\bar{Q} (\bar{Q} - \lambda_b \bar{M})^{-1} \left(1 + \frac{d \ln \bar{Q}}{d \ln F} \right) \right]. \quad (100)$$

Since by definition \bar{M} and \bar{Q} are on the hyperbola, $\bar{M} d\bar{M}/dF = \bar{Q} d\bar{Q}/dF$ holds; and then, by differentiating Eq. (65), the factor in brackets in Eq. (100) can be shown to simplify to $[-N_i^2/(\bar{Q} - \lambda_b \bar{M})^2]$, so that ΔQ is given by

$$\Delta Q = \Delta \bar{Q} [1 - \beta N_i^2/(\bar{Q} - \lambda_b \bar{M})^2], \quad (101)$$

with

$$\beta \equiv (\tau_0/K\tau_d)(1 - \Delta \hat{N}/2\Delta \bar{Q}). \quad (102)$$

The condition for the hyperbola is that the second term in brackets in Eq. (101) be small compared with unity. This condition will fail as $(\bar{Q} - \lambda_b \bar{M})$ approaches zero. It is easily seen that this quantity is zero for $\mu_p p = \mu_n n = (\mu_n \mu_p)^{1/2} n_i$, or at the point of minimum conductivity, at which the electron and hole drift currents are equal. With $\mu_n/\mu_p > 1$, this point occurs on branch I for n -type material and on branch II for p type. In the latter case, the solution for drift only may be extended past the conversion point; a solution for branch II may be joined there to the solution for branch I since there is an initial decrease in conductivity past the conversion point which is now consistent with the increasing $|F|$ required by Poisson's equation.

The boundary of the recombination front may be specified by the β for which the ΔQ given by Eq. (101) is zero:

$$\beta = (\bar{Q} - \lambda_b \bar{M})^2 / N_i^2. \quad (103)$$

Then,

$$\bar{\Sigma} \equiv (1 + \alpha) \Sigma_m, \quad 0 < \alpha \ll 1 \quad (104)$$

with Σ_m the minimum-conductivity value given by Eq. (69), defines a variable α for which Eq. (103) determines a value. Because the length of the de-

pletion drift region is proportional to Σ_m^{-1} for $N_i \ll 1$, this value is the relative extent of the front. Introduce, for convenience, the variable⁶⁸ $\gamma \equiv \pm \beta^{1/2}$ so that Eq. (103) is

$$\bar{Q} - \lambda_0 \bar{M} \equiv \gamma N_i, \quad |\gamma| \ll 1. \quad (105)$$

With $\bar{\Sigma}$ given in terms of \bar{M} and \bar{Q} by Eq. (63), by differentiating Eqs. (63) and (105) with respect to γ , $\bar{\Sigma}$ may be expanded in powers of γ . From $d\bar{\Sigma}/d\gamma = N_i^2 \gamma / \bar{\Sigma}$ and the next derivative follows

$$\bar{\Sigma} = [1 + \frac{1}{2}(N_i/\Sigma_m)^2 \gamma^2] \Sigma_m, \quad (106)$$

and the second term in brackets is α . With $\gamma^2 = \beta$ evaluated from Eq. (102) for minimum conductivity, use also of Eq. (63) and

$$Q_m/N_i = \lambda_b M_m/N_i = \lambda_b (1 - \lambda_b^2)^{-1/2}$$

gives the result for α of Eqs. (75) and (76).

APPENDIX B: RELAXATION-CASE CONCENTRATIONS WITH UNIFORM TRAPPING

The condition $\mathcal{R} = 0$ gives from Eqs. (6) and (7) the equations relating concentration increments,

$$\begin{aligned} \Delta n &= \frac{(n_0 + n_1) \Delta \hat{n}}{\mathfrak{X} - \hat{n}_0 - \Delta \hat{n}} = \frac{n_0 \Delta \hat{n}}{\mathfrak{X}^* - \hat{n}_0 \Delta \hat{n} / \mathfrak{X}}, \\ \Delta p &= - \frac{(p_0 + p_1) \Delta \hat{n}}{\hat{n}_0 + \Delta \hat{n}} = - \frac{p_0 \Delta \hat{n}}{\mathfrak{X}^* + (1 - \hat{n}_0 / \mathfrak{X}) \Delta \hat{n}}, \\ \Delta p &= - \frac{p_0 \Delta n}{n_0 + \Delta n}, \end{aligned} \quad (107)$$

any two of which are independent. In the first two equations, \mathfrak{X}^* is the capture concentration³ defined by Eq. (58). For depletion of majority holes in a p -type semiconductor, consider the first equation, from which Δn after recombination equals n_0 for

$$\Delta \hat{n} = \mathfrak{X}^* / (1 + \hat{n}_0 / \mathfrak{X}) \approx \mathfrak{X}^*, \quad (108)$$

the approximation being within a factor of 2 because of $0 < \hat{n}_0 / \mathfrak{X} < 1$. A similar result holds for the concentration increment $-\Delta \hat{n}$ of trapped holes in the

n -type case, as may easily be verified from the second equation. Note that \mathfrak{X}^* is symmetrically defined with respect to the fractions of all traps that are empty and filled. Thus, pronounced majority-carrier depletion requires that the concentration increment of traps filled by minority carriers be well in excess of \mathfrak{X}^* after recombination.

Consider now unipolar injection of minority electrons in concentration Δn_1 . The space charge is given by its initial value $-e \Delta n_1$, so that with Eq. (107)

$$\begin{aligned} -\Delta n_1 &= \Delta p - \Delta n - \Delta \hat{n} \\ &= - \left(1 + \frac{(n_0 + p_0) \mathfrak{X} + (n_0 + n_1 - p_0 - p_1) \Delta \hat{n}}{\mathfrak{X} \mathfrak{X}^* + (\mathfrak{X} - 2\hat{n}_0) \Delta \hat{n} - \Delta \hat{n}^2} \right) \Delta \hat{n} \end{aligned} \quad (109)$$

follows. By solving a cubic equation, $\Delta \hat{n}$ and then $\Delta p - \Delta n$ may be found in terms of Δn_1 . Consider, however, the case $\Delta \hat{n} \ll \mathfrak{X}^*$. This would not be one of appreciable hole depletion, and transition in the $\Delta M - \Delta Q$ plane would be to branch II of the hyperbola. For this case, Eq. (109) gives

$$\Delta \hat{n} \approx \frac{\Delta n_1}{1 + (p_0 + n_0) / \mathfrak{X}^*} \quad (110)$$

and

$$\Delta p - \Delta n \approx - \frac{p_0 + n_0}{\mathfrak{X}^*} \Delta \hat{n} \approx \frac{-\Delta n_1}{1 + \mathfrak{X}^* / (p_0 + n_0)}. \quad (111)$$

As shown in Fig. 1, the transition is accordingly not along a horizontal line of constant ΔQ , but is directed upward to a point on branch II, with ΔQ smaller in magnitude by the trapping factor in Eq. (111), which is N^* defined by Eq. (59). Sufficiently large Δn_1 will provide transition to a point on branch I. While such transition entails $\Delta \hat{n} \gg \mathfrak{X}^*$, Eq. (111) can nevertheless provide an estimate of how large Δn_1 must be: With $(\Delta p - \Delta n)$ equal to $(n_0 - p_0)$ at the conversion point, the estimate given by Eq. (60) is obtained.

¹W. van Roosbroeck, Phys. Rev. **123**, 474 (1961); Bell Telephone System, Tech. Publ. Monographs, No. 3997 (1961).

²For definition and discussion of τ_0 see Sec. II A and Ref. 3.

³W. van Roosbroeck, Bell System Tech. J. **39**, 515 (1960); Phys. Rev. **119**, 636 (1960); Bell Telephone System, Tech. Publ. Monographs, No. 3586 (1960).

⁴Italics in the text denote coined or specified usages.

⁵For differing mobilities, there are also solutions of a third type that are transitional between solutions of the principal types and which apply for values of τ_0 of order τ_0 over a certain relative range equal to the mobility ratio. See Ref. 1.

⁶For a brief presentation, see W. van Roosbroeck and H. C. Casey, Jr., in *Proceedings of the Tenth International Conference on the Physics of Semiconductors, Cambridge,*

Mass., 1970, edited by S. P. Keller, J. C. Hensel, and F. Stern (U.S. AEC Division of Technical Information, Springfield, Va., 1970), p. 832.

⁷H. J. Queisser, H. C. Casey, Jr., and W. van Roosbroeck, Phys. Rev. Letters **26**, 551 (1971).

⁸These solutions of the two principal types have been verified by computer [J. L. Scales and A. L. Ward, J. Appl. Phys. **39**, 1692 (1968)]. For a large-signal pulse, the local field and ambipolar mobility in the pulse do not properly apply in the comparisons of Fig. 8 of this reference.

⁹See Fig. 2 of Ref. 1.

¹⁰To linearize the differential equations of Ref. 1 for drift of an injected pulse required the strong condition of excess concentrations of both carriers small compared with the equilibrium values, a condition requiring, in practice, not too strongly extrinsic material.

- ¹¹W. Shockley, Bell System Tech. J. **28**, 435 (1949).
- ¹²For the theory of effects of recombination and generation on p - n junction characteristics see C.-T. Sah, R. N. Noyce, and W. Shockley, Proc. IRE **50**, 1228 (1957); O. V. Konstantinov, G. V. Tsarenkov, and A. L. Éfros, Fiz. Tekhn. Poluprov. **1**, 1739 (1967) [Sov. Phys. Semicond. **1**, 1443 (1968)].
- ¹³W. Shockley and R. C. Prim, Phys. Rev. **90**, 753 (1953).
- ¹⁴G. C. Dacey, Phys. Rev. **90**, 759 (1953).
- ¹⁵N. F. Mott and R. W. Gurney, *Electronic Processes in Ionic Crystals* (Oxford U.P., New York, 1940), p. 172.
- ¹⁶M. A. Lampert, Proc. IRE **45**, 1781 (1962).
- ¹⁷G. G. Roberts and R. H. Tredgold, J. Phys. Chem. Solids **24**, 1263 (1963); **25**, 1349 (1964).
- ¹⁸A. Rose, *Concepts in Photoconductivity and Allied Problems* (Interscience, New York, 1963).
- ¹⁹R. H. Tredgold, *Space Charge Conduction in Solids* (Elsevier, New York, 1966), Chap. 3.
- ²⁰M. A. Lampert and P. Mark, *Current Injection in Solids* (Academic, New York, 1970).
- ²¹*Injection Phenomena*, Vol. 6 of *Semiconductors and Semimetals*, edited by R. K. Willardson and A. C. Beer (Academic, New York, 1970).
- ²²K. L. Ashley and A. G. Milnes, J. Appl. Phys. **35**, 369 (1964).
- ²³W. H. Weber and G. W. Ford, Solid-State Electron. **13**, 1333 (1970).
- ²⁴This usage is employed in Ref. 7.
- ²⁵P. Langevin, Ann. Chim. Phys. **28**, 289 (1903); **28**, 433 (1903); see also W. R. Harper, Proc. Cambridge Phil. Soc. **28**, 219 (1932); **31**, 429 (1935); Phil. Mag. **18**, 97 (1934); **20**, 740 (1935).
- ²⁶M. Lax, Phys. Rev. **119**, 1502 (1960).
- ²⁷N. Holonyak, Jr. (private communication); Proc. IRE **50**, 2421 (1962).
- ²⁸J. S. Moore, C. M. Penchina, N. Holonyak, Jr., M. D. Sirkis, and T. Yamada, J. Appl. Phys. **37**, 2009 (1966).
- ²⁹B. G. Streetman, M. M. Blouke, and N. Holonyak, Jr., Appl. Phys. Letters **11**, 200 (1967).
- ³⁰J. S. Moore, N. Holonyak, Jr., and M. D. Sirkis, Solid-State Electron. **10**, 823 (1967), and references therein.
- ³¹See Ref. 28. This was with cobalt-compensated Si.
- ³²G. G. Roberts, Phys. Status Solidi **27**, 209 (1968).
- ³³The formulation has formal similarity to that for a one-carrier case with trapping given in Ref. 19, Sec. 3, 5.
- ³⁴With GaAs, intrinsic resistivity is favorably high, and fairly short lifetimes are associated with direct band-to-band recombination. GaP has even higher intrinsic resistivity. See Sec. III C and T. Kinsel and I. Kudman, Solid-State Electron. **8**, 797 (1965); Y. P. Varshni, Phys. Status Solidi **19**, 459 (1967); **20**, 9 (1967).
- ³⁵N. F. Mott, Advan. Phys. **16**, 49 (1967).
- ³⁶A. I. Gubanov, *Quantum Electron Theory of Amorphous Conductors* (Consultants Bureau, New York, 1965).
- ³⁷*Proceedings of the Symposium on Semiconductor Effects in Amorphous Solids*, edited by W. Doremus (North-Holland, Amsterdam, 1970).
- ³⁸*Amorphous and Liquid Semiconductors*, edited by N. F. Mott (North-Holland, Amsterdam, 1970).
- ³⁹K. W. Böer, Phys. Status Solidi **34**, 721 (1969); **34**, 733 (1969); Ref. 37, p. 444; Ref. 38, p. 583.
- ⁴⁰M. H. Cohen, in Ref. 37, p. 432; Ref. 38, p. 391.
- ⁴¹R. S. Allgaier, J. Vac. Sci. Technol. **8**, 113 (1971).
- ⁴²A. K. Jonscher, J. Vac. Sci. Technol. **8**, 135 (1971).
- ⁴³J. I. Pankove, *Optical Processes in Semiconductors* (Prentice-Hall, Englewood Cliffs, N.J., 1971), Chap. 14.
- ⁴⁴W. van Roosbroeck, Bull. Am. Phys. Soc. **16**, 348 (1971).
- ⁴⁵W. van Roosbroeck (unpublished).
- ⁴⁶H. J. Hovel, Appl. Phys. Letters **17**, 141 (1970).
- ⁴⁷H. J. Hovel and J. J. Urgell, J. Appl. Phys. **42**, 5076 (1971).
- ⁴⁸Results of the present derivation also follow expeditiously from Eqs. (19) of Ref. 1. Notation of this reference is employed.
- ⁴⁹Thus, analysis in the Appendix of Ref. 32 is for the intrinsic case.
- ⁵⁰The strong condition specified in Ref. 10 is required.
- ⁵¹In the lifetime case, local neutrality results in ambipolar diffusion, and the equilibrium diffusivity divided into the square of the diffusion length gives τ_0 .
- ⁵²It is also defined by equality level between the majority-carrier band edge and the Fermi level.
- ⁵³Note that replacing τ_0 by τ_d in the diffusion length, $(kT\mu\tau_0/e)^{1/2}$, gives L_D .
- ⁵⁴Near an injector, where M'_0 is sufficiently large, filling of traps may cause an increase in τ'_0 , as may be derived from Eq. (7).
- ⁵⁵For unequal mobilities, the equilibrium ratio is multiplied by $(n+p)(\mu_n n_0 + \mu_p p_0)/(n_0 + p_0)(\mu_n + \mu_p)$, so that along the hyperbola for n -type or p -type material, it ranges from the equilibrium value to a limiting value under minority-carrier injection that is, respectively, larger or smaller by the factor μ_n/μ_p .
- ⁵⁶The various parameters for this case are $Q_0=0.98$, $N_i=0.198$, $\lambda_0=1.60$, and $\lambda_1=0.82$. Note that only one independent parameter is actually involved.
- ⁵⁷Expansions in X obtained by including the drift term and using M for branch I from Eqs. (33) are the same as Eqs. (41) except for terms of higher order, which depend on λ_0 and λ_1 as well as an ΔQ_b and F_a .
- ⁵⁸The start of predominant drift is generally not exactly at X_1 but where M is sufficiently smaller than its branch-point value so that the diffusion term is negligible. Specifying that the local value of this term, $d\Delta Q/dX = d^2F/dX^2$, calculated under the assumption of drift only, be small compared with $|F_a|$ gives $|F_a|d\Delta Q/dX \approx M^2(M+1) \ll F_a^2$ from the first of Eqs. (33) and (42) and their X derivatives.
- ⁵⁹The length from injector to termination would of course be established first and the bias voltage adjusted accordingly.
- ⁶⁰It would be a Debye length if the lifetime case were applicable.
- ⁶¹The possible alternative of relatively slight trapping need not be considered.
- ⁶²An estimate in Ref. 7 shows consistency of V_k with barrier-region lifetime and transit time of injected carriers.
- ⁶³H. C. Casey, Jr. and M. B. Panish, Trans. AIME **242**, 406 (1968).
- ⁶⁴Measurements were at 295 °K, as reported in Ref. 7. Use of values of n_0 and n_i for this temperature rather than for 300 °K largely accounts for various numbers in the present Sec. III differing from ones in Sec. 3 of Ref. 6.

⁶⁵In early experiments by T. M. Buck (private communication), a similar sample (but with a Ga end contact) gave the sublinear range, while one from a nearby region of the same crystal did not.

⁶⁶H. C. Casey, Jr. and F. Ermanis (unpublished).

⁶⁷Though well suited for the junction case of Sec. II D2,

the independent variable W would be less convenient here than F .

⁶⁸By considering $dM/d\gamma$ along the hyperbola short of the minimum-conductivity point, $\gamma < 0$ can be shown to hold for p type, and $\gamma > 0$ for n type.

Valence-Band Structure of PtSb₂

D. H. Damon,* R. C. Miller, and P. R. Emtage

Westinghouse Research Laboratories, Pittsburgh, Pennsylvania 15235

(Received 28 June 1971)

The low-temperature galvanomagnetic properties of p -type PtSb₂ are reported for magnetic fields up to 60 kG, using samples with extrinsic current-carrier densities from 6×10^{16} to 1.5×10^{19} cm⁻³. From the low-field properties and the Shubnikov-de Haas oscillations it is found that the valence-band maxima are six ellipsoids on $\langle 100 \rangle$ axes, the principal inertial effective masses being in the ratio 0.61 : 1 : 1.64, the least cyclotron mass $(0.168 \pm 0.005)m$, and scattering close to isotropic. The band parameters are found to be independent of the energy of the current carrier, suggesting a direct band gap greater than 0.4 eV; cf. indirect band gap of about 0.1 eV. The ratio of effective masses was obtained by analyzing small beats in the amplitude of the oscillations in the resistivity.

I. INTRODUCTION

In this paper we report the valence-band structure of platinum antimonide PtSb₂, a narrow-band-gap semiconductor of the pyrite structure. A number of inquiries into the preparation, transport properties, optical properties, and band structure of this material have been published.¹⁻⁶ Here we give measurements of the magnetoresistance and Hall coefficient of p -type PtSb₂ at low temperatures 1.3–4.2 °K, in magnetic fields up to 60 kG, for samples with extrinsic carrier concentrations between 6×10^{16} and 1.5×10^{19} cm⁻³.

From prior work² we know the valence-band maxima of PtSb₂ to be centered on the $\langle 100 \rangle$ axes. The pyrite structure is of cubic class T_h , invariant under twofold rather than fourfold rotations about the principal axes. From the point of view of this paper the most interesting consequence of this symmetry is that a band maximum on one of the principal axes, at $[k00]$ say, is characterized by three unequal principal effective masses (m_1, m_2, m_3). Masses at the equivalent stationary points are obtained by a cyclic permutation of the indices; e.g., at $[0 \pm k 0]$ the effective masses are (m_3, m_1, m_2). One result of this symmetry is that when a current flows in the $[100]$ direction the transverse magnetoresistances with $H \parallel [010]$ and with $H \parallel [001]$ need not be the same, and generally are not.

The band gap of PtSb₂ is small, about 0.10 eV,^{2,3} so it would not be surprising to find that the effective masses are dependent on the Fermi level. A calculation by one of the authors⁶ suggests that the

warping of the bands may be unusually large in this material. Our investigation was therefore carried out over the wide range of carrier concentrations noted above; no sign of a dependence of any of the effective masses on the energy of the holes was found.

Section III is rather long and involved. We briefly outline this discussion so as to indicate clearly which results we believe to be the most important and what conclusions may be drawn from them. We first examined that part of the low-field magnetoresistance that is quadratic in the field strength. From the data one can find the ratio $m_1/\tau_1 : m_2/\tau_2 : m_3/\tau_3$, m_i and τ_i being principal effective masses and relaxation times. The results provide a test of the multivalley model and preliminary values of the effective-mass ratios if the relaxation time is presumed isotropic. The interpretation of these results is made difficult by the presence of a negative magnetoresistance in most of the samples. At high fields Shubnikov-de Haas oscillations are observed in both the magnetoresistance and the Hall coefficient. We obtain the periods and amplitudes of these oscillations as a function of carrier concentration, temperature, and orientation of the magnetic field. Each period is inversely proportional to a stationary area of the Fermi surface measured normal to the direction of the field; for a general field direction the six valence-band maxima have three distinct stationary areas. The observed oscillations are due to the smallest of these areas, since oscillations due to the greater areas are more strongly damped by